expressed in mouse spermatogonia and somatic Sertoli cells but not in post meiotic germ cells (Kwon et al., 2004a). By contrast, UCH-L3 is detected mainly in spermatocytes and round spermatids (Kwon et al., 2004a). These two isozymes are considered to play important roles in the labeling/targeting of abnormal proteins for degradation via the ubiquitin-proteasome system (Wilkinson, 2000).

The gracile axonal dystrophy (*gad*) mouse is an autosomal recessive spontaneous mutant carrying an intragenic deletion of the gene encoding UCH-L1 (*Uchl1*). *gad* mice do not express UCH-L1 and thus are comparable to a *Uchl1* null mutant (Yamazaki et al., 1988; Saigoh et al., 1999). We recently showed that *gad* mice are resistant to the germ cell apoptosis during the first round of spermatogenesis (Kwon et al., 2005) and are also resistant to cryptorchid-induced testicular germ cell apoptosis (Kwon et al., 2004b). The expression of the apoptotic proteins p53, Bax, and caspases-3 was significantly lower in the immature testes, and the expression of both antiapoptotic and prosurvival proteins such as Bcl-2, Bcl-xL, XIAP, pCREB, and BDNF was significantly higher in *gad* mice following experimental cryptorchidism (Kwon et al., 2004b). These data prompted our hypothesis that UCH-L1 may be an important regulator of apoptosis during spermatogenesis. Experiments toward this end may provide additional evidence that UCH-L1 regulates spermatogenesis.

Our present report presents the characterization of the male sterility phenotype and the quantitation of apoptotic spermatocytes in *Uchl1* transgenic (Tg) mice. Constitutive expression of UCH-L1 in the testis results in a blockade of spermatogenesis at the pachytene stage of spermatocytes due to an increase in the number of apoptotic spermatocytes. These results indicate that excess UCH-L1 affects spermatogenesis during meiosis and, in particular, induces apoptosis in primary spermatocytes.

MATERIALS AND METHODS

Animals

We have previously described the Tg *Uchl1* mice carrying a 0.7-kb FLAG-tagged mouse *Uchl1* cDNA with the human translation elongation factor-1α (*EF-1α*) promoter (Osaka et al., 2003). Tg mice were identified by PCR analysis of tail DNA using specific primers (forward: ex6F, 5′-ATCCAGGCGGCCCATGACCTC-3′; reverse: ex9R, 5′-AGCTGCTTTGCAGAGAGCCA-3′). The *gad* mouse is an autosomal recessive mutant that was obtained by crossing CBA and RFM mice (Saigoh et al., 1999). All strains were maintained at our institute. To corroborate fertility disturbances in UCH-L1 Tg mice, a subset of the mice was continuously mated with wild-type C57BL/6J mice. The mating of two heterozygous Tg males with non-Tg females did not yield offspring until the age of 6 months despite grossly normal appearance. This was also the case for the mating of four heterozygous Tg females with non-Tg males. Their non-Tg littermates sired offspring normally. Finally, all six Tg mice were infertile, but they did not exhibit any apparent neurological phenotype during adulthood. Controls included nontransgenic (non-Tg) littermates and UCH-L1-deficient *gad* mice (Saigoh et al., 1999). Mice were sacrificed by cervical dislocation before tissue collection. Animal care and handling were in accordance with institutional regulations for animal care and were approved by the Animal Investigation Committee of the National Institute of Neuroscience, National Center of Neurology and Psychiatry of Japan.

mRNA Isolation, and Exogenous *Uchl1* Expression Measured by Quantitative Real-Time RT-PCR

Total RNA from testes was isolated using the Trizol reagent (Gibco BRL Life Technologies, Bethesda, MD) and purified following the manufacturer's instructions. Real-time quantitative RT-PCR primer pairs flanking introns were used to specifically amplify transgene products, and their sequences were: forward, 5′-ATTT-CAGGTGTCGTGAGGAA-3′; and reverse, 5′-CCCAC-GTGGGAGACCTGATA-3′. Real-time quantitative PCR products, from 0.25–2.5 ng of reverse-transcribed cDNA samples, were detected using an ABI Prism, 7700 system (Applied Biosystems) as described previously (Aoki et al., 2002). β-Actin and GAPDH were used as endogenous controls. Results are expressed as the ratio of the mRNA level of the transgene to that of β-actin or GAPDH. As an external standard for quantitative analysis, the cDNA of the 3′-noncoding region of mouse *Uchl1* cDNA (covering the RT-PCR primers) was cloned and inserted into a pcDNA3 vector, purified, precisely quantified, and serially diluted 10-fold to 10 copies/μl. Standard curves were determined using linear regression analysis of the Ct values relative to plasmid copy numbers. In each real-time quantitative PCR assay, a 10-fold serially diluted cDNA template series was added to construct a standard curve for copy number. Each sample was analyzed in triplicate, and copy numbers were determined from each corresponding standard curve by the ratio of Tg *UCH-L1* to mouse *Uchl1*.

Histological Observations, Immunohistochemistry, and Immunofluorescence

Morphological studies were performed on six male controls and two male Tg mice (Tg21 and Tg22, both 6 months old). The two control groups consisted of three non-Tg wild-type C57BL/6J mice, 6 months old, littermates, and three *gad* mice, age 4 months. Testes were fixed in 4% paraformaldehyde for 24 hr and embedded in paraffin. Serial 5-μm sections were used for histology after hematoxylin–eosin staining as well as for immunohistochemistry and the TUNEL assay. Primary monoclonal or polyclonal antibodies against the following proteins were used at the final dilutions indicated: UCH-L1 (RA95101, Ultraclone, Lucigen, Middleton, WI, 1:2,000), FLAG (FM2, Sigma, St. Louis, MO, 1:500), PCNA (PC10, Santa Cruz Biotechnology, Santa Cruz, CA, 1:200), PCNA (Clone 24, BD Transduction

Laboratory, Lexington, KY, 1:2,000), vimentin (Zymed, 1:100), and ubiquitin (Dako, Carpenteria, CA, 1:400). For controls, the primary antibody was replaced with normal rabbit serum or was omitted (these controls always yielded negative staining). For immunofluorescence studies, secondary antibodies were anti-mouse-Cy3 or -FITC or anti-rabbit-conjugated-Cy3 or -FITC (Jackson ImmunoResearch, West Grove, PA, 1:500).

TUNEL Assay

TUNEL staining was performed according to the original protocol, with modifications (Harada et al., 2004). The number of apoptotic cells was determined by counting positively stained nuclei in 30 tubule cross-sections per testis section in each testis (Kwon et al., 2004b). For clarity and brevity, we also counted all the TUNEL-stained cells within the entire cell population of testicular tubules in each section. In addition, we also counted the apoptosis-positive tubules (i.e., tubules containing at least one apoptotic cell) in each testis.

Western Blotting

Protein lysates were prepared from mouse testes as described (Kwon et al., 2004b). Approximately 20 μg of total protein was loaded per lane on 15% SDS–PAGE gels. Primary antibodies (diluted as indicated) were used to detect the following proteins: UCH-L1 (RA95101, 1:5,000), FLAG (FM2, Sigma, 1:2,000), Bcl-2 (Cell Signaling, Beverly, MA, 1:1,000), caspase-3 (Cell Signaling, 1:400), polyubiquitin (FK2 clone, Medical & Biological Laboratory, Nagoya, Japan, 1:1,000), and monoubiquitin (U5379, Sigma, 1:1,000). Blots were further incubated with peroxidase-conjugated goat anti-mouse IgG or goat anti-rabbit IgG (1:5,000; Pierce, Rockford, IL) for 1 hr at room temperature. Immunoreactions were visualized using the SuperSignal West Dura extended duration substrate (Pierce) and analyzed with a ChemiImager (Alpha Innotech, San Leandro, CA). ChemiImager data were analyzed using AlphaEase software (Alpha Innotech) to yield the relative level of each protein.

RESULTS

Sterile Phenotype of *Uchl1* Tg Mice

We initially attempted to overexpress *Uchl1* in neurons using a Tg construct containing the *EF-1α* promoter (Mizushima and Nagata, 1990). The transgene was also strongly expressed in gonads as well as other Tg mice via the same promoter (Furuchi et al., 1996). We obtained six Tg mice having high transgene copy number, each of which most likely carried the transgene in a unique genomic location (see below). Four of these mice were females (Tg11, Tg12, Tg43, Tg81) and two were males (Tg21 and Tg22). Unexpectedly, all of these Tgs were sterile. Thus, it was not possible to maintain Tg lines during the course of these experiments. However, in addition to the sterile phenotype, the six independent Tg mice showed a similar pattern of *Uchl1* transgene expression and common pathological defects, the latter being limited to the testes or ovaries. The Tg loci were generated by random integration rather than by site-specific recombination, and thus the animals produced by our Tg procedure usually had more than one transgene integrated at each chromosomal site (Kroll and Amaya, 1996). Therefore, in each of the six Tg mice, the transgene most likely integrated into a different genomic site, raising the possibility of different position-dependent effects. Our data showed that we obtained multiple animals with similar patterns or levels of *Uchl1* transgene expression and with common pathological defects, suggesting the phenotypes reflect position-independent expression (i.e., independent of the position of transgene insertion). Thus, these Tg mice had similar infertile phenotypes that may be attributed to the overproduction of UCH-L1. Numerous gene inactivation studies have identified gene products involved in male fertility, but in most cases female reproduction was unaffected or weak damaged (Yuan et al., 2000). However, both male and female *Uchl1* Tg mice were infertile, although there were clear differences in germinal cell maturation, suggesting that UCH-L1 is required for both spermatogenesis and oogenesis. Therefore, six independent Tg founders, notably two males (Tg21 and Tg22), were analyzed in our present study.

The mating of two heterozygous Tg males with non-Tg females did not yield offspring until the age of 6 months, despite grossly normal appearance. This was also the case for the mating of four heterozygous Tg females with non-Tg males. Their non-Tg littermates sired offspring normally. At autopsy, the testes of both Tg21 and Tg22 appeared grossly smaller than those of non-Tg mice. The testes weight of Tg21 (77 mg) and Tg22 (70 mg) was only 42% and 38%, respectively, relative to non-Tg males (183 ± 16 mg), demonstrating that mice overexpressing UCH-L1 display profoundly defective testis development.

Expression Levels of the *Uchl1* Transgene

We used RT-PCR and primers specific for the *Uchl1* transgene to compare transgene expression levels in the testes or ovaries of the six Tg mice. There was some variation between animals (Fig. 1A). All the Tgs expressed a similar level of endogenous *Uchl1* mRNA (Fig. 1A); quantitation of absolute Tg *Uchl1* copy numbers using real-time quantitative RT-PCR showed that all six Tgs expressed 2.9–6.8-fold more *Uchl1* transgene mRNA compared with endogenous mRNA (4.5, 3.6, 6.2, 3.7, 2.9, and 6.8 for Tg21, Tg22, Tg11, Tg12, Tg43, and Tg81, respectively). Relative UCH-L1 protein expression was similar among four of the Tgs (76.1 ± 5.2; Fig. 1B) but was somewhat higher in Tg 21 (100) and Tg81 (106.2). The average level of endogenous UCH-L1 expression in Tg mice was ~91% relative to non-Tg mice (Fig. 1B).

Immunohistochemistry of testicular sections using an antibody against FLAG revealed that exogenous UCH-L1 localized mainly in spermatogonia and Sertoli cells (Fig. 2E), similar to the localization of endogenous UCH-L1 (Fig. 2A). Endogenous UCH-L1 localized to both the cytoplasm and nucleus of spermatogonia and Sertoli

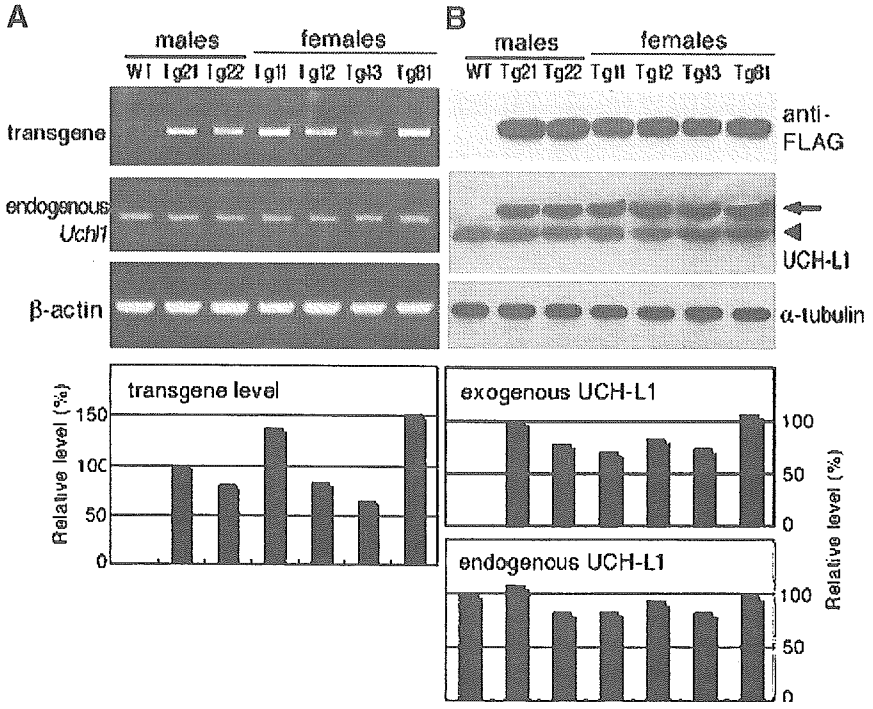

Fig. 1. Expression of transgenic ubiquitin carboxyl-terminal hydrolase 1 (UCH-L1) in the testes of Tg21 and Tg22 male mice. **A**: Transgenic *Uchl1* mRNA levels in the testes. RT-PCR showed high levels of *Uchl1* transgene mRNA in both Tg21 and Tg22 as well as in all ovaries from four female Tg mice. All Tg mice had a normal level of endogenous *Uchl1* mRNA. The relative expression level is indicated below each lane (as a percentage, scaled to β-actin in each lane). **B**: Western blot analysis of testicular or ovarian lysates. Both endogenous and exogenous UCH-L1 were detected with anti-UCH-L1, whereas exogenous UCH-L1 was specifically detected by anti-FLAG. Exogenous UCH-L1 (arrow) is slightly larger than endogenous UCH-L1 (arrowhead). WT, non-Tg wild-type.

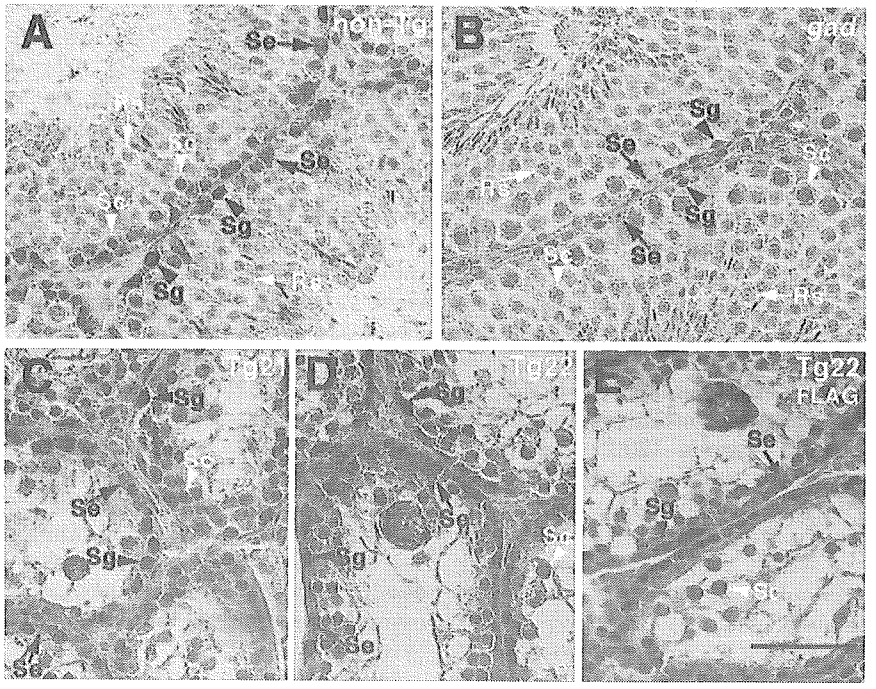

Fig. 2. Immunostaining of FLAG and UCH-L1 in *Uchl1* Tg mice shows high levels of UCH-L1 in testicular tubules. UCH-L1 immunostaining is clearly present in spermatogonia (Sg) and Sertoli cells (Se) of a non-Tg mouse (**A**) but not in a *gad* mouse (**B**). In contrast, in the testes of two Tg males, the most intense UCH-L1 immunoreactivity occurs predominantly in spermatogonia (Sg, arrowheads) and Sertoli cells (Se, arrows) but not in the primary spermatocytes (Sc, white arrowheads; **C**, Tg21; **D**, Tg22). **E**: Immunostaining of FLAG confirmed the transgene-derived UCH-L1 proteins in spermatogonia (Sg, arrowheads) and Sertoli cells (Se, arrows) but not in the primary spermatocytes (Sc, white arrowheads; Tg22). Magnification: ×400. Scale bar, 50 μm.

cells in the testes of non-Tg males; however, localization was not apparent around pachytene spermatocytes or round, elongated spermatids (Fig. 2A). This distribution of UCH-L1 is in good agreement with previous reports (Kon et al., 1999; Kwon et al., 2004a). Compared with non-Tg males, overexpression of UCH-L1 in seminiferous tubules of Tg males (Tg21 and Tg22) occurred predominantly in spermatogonia and Sertoli cells, and was weakly positive or negative in spermatocytes (Fig. 2C,D). These data coincided with strong induction of the *Uchl1* transgene. Tg mice expressed a higher level of total UCH-L1 (both endogenous and exogenous), suggesting a correlation between excess UCH-L1 and sterility.

Morphological Examination

Histopathological analysis of testes from 6-month-old Tg21 and Tg22 revealed terminal loss of differentiated germ cells and a large number of pachytene spermatocytes that had degenerated (with condensed nuclei and giant cells) and been sloughed off, forcing an altered structure of the seminiferous tubules such that they appeared almost empty (Fig. 3A). The deformed seminiferous tubules also contained numerous arrested spermatocytes (Fig. 3A, arrowheads) and multinucleated giant cells (arrows). In contrast, the seminiferous tubules of *gad* mice were nearly intact, as in non-Tg males (data not shown). In non-Tg males, seminiferous tubules containing elongated spermatids in the inner layer were readily detected (data not shown), whereas these tubules were scarcely detectable in Tg21 (Fig. 3A) and Tg22. On the other hand, the four female Tg mice displayed a variety of phenotypes, including an increased number of apoptotic oocytes and granulosa cells relative to non-Tg females, leading to infertility (data not shown).

In non-Tg (Fig. 3B) and *gad* mice (Fig. 3C), only a few TUNEL-positive cells were identified, located at the periphery of the tubule. However, many fewer TUNEL-positive cells were detected in the Tg males (Fig. 3D,E), and cell morphology indicated that most of these positive cells were primary spermatocytes. However, neither the TUNEL assay nor microscopy revealed evidence of apoptosis in spermatogonia or Sertoli cells. We quantitatively assessed germ cell apoptosis in Tg, non-Tg, and *gad* mice by calculating the number of apoptotic cells per tubules in each testis. This value was 25 times higher in Tg testes compared with non-Tg or *gad* testes (the averages ± SD were as follows: 553 ± 72, n = 2 in Tg testes; 22 ± 4.2, n = 3 in non-Tg; and 21 ± 5.3, n = 3 in *gad*). The percentage of apoptosis-positive tubules in Tg testes was also significantly higher than in non-Tg or *gad* mice (the averages ± SD were as follows: 95.3 ± 2.7, n = 2 in Tg testes; 7.4 ± 2.2, n = 3 in non-Tg; and 7.1 ± 1.8, n = 3 in *gad*).

A control section of caput epididymis, an androgen-dependent organ, from same Tg mice was investigated. No UCH-L1 overexpressing was detected, and no pathological symptoms could be observed in the epididymis (data not shown).

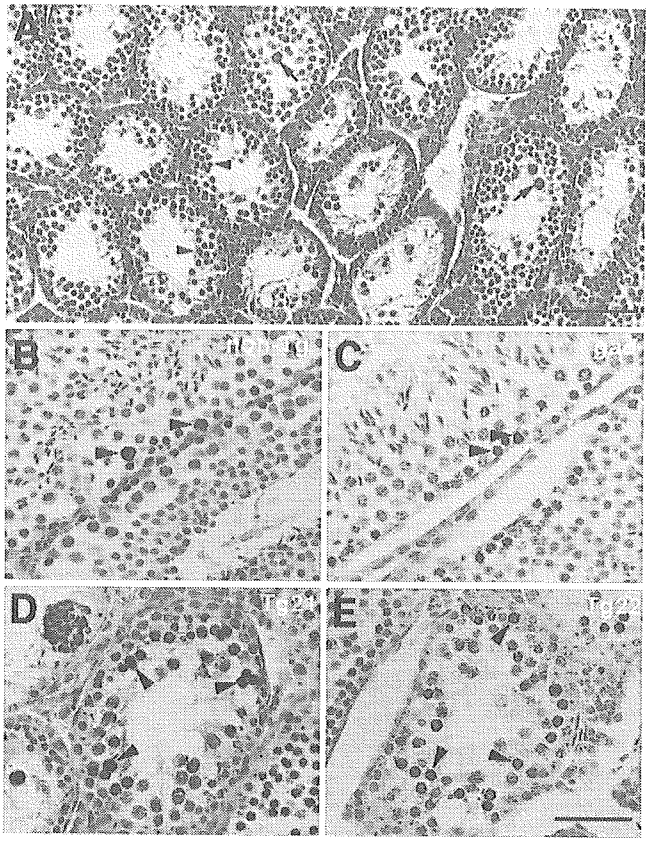

Fig. 3. Histopathology and TUNEL assay in situ. **A**: Hematoxylin–eosin staining of testis sections from the Tg21 male mouse shows defective spermatogenesis. Arrowheads indicate arrested spermatocytes and arrows indicate giant cells. Round spermatocytes and spermatids were rarely observed. **B–E**: Examples of TUNEL-positive cells characterized by the robust deposition of the reddish brown reaction product in sections of testis from non-Tg (B), *gad* (C), and Tg mice (D, Tg21; E, Tg22). Sections were counterstained with hematoxylin. A large number of TUNEL-positive cells were clearly observed at the periphery of the seminiferous tubule (arrowheads) in Tg21 (D) and Tg22 (E), whereas a lesser number of positives were apparent in non-Tg (B) or *gad* mice (C). Most of these positive cells appeared to be primary spermatocytes. Magnification: (A) ×100; (B–E) ×400. Scale bar in (A) 200 μm; (E) 50 μm.

UCH-L1 Relates to the Expression of PCNA

PCNA expression is associated with cell proliferation and DNA synthesis during S phase of the cell cycle and DNA repair in non-dividing cells (Kelman, 1997; Toschi and Bravo, 1988). Unlike UCH-L1, which is abundant in brain, PCNA is not detectable in the central nervous system (Saigoh et al., 1999; Williams et al., 2002). In the testis, PCNA is expressed in germ cells and Sertoli cells, and the nuclear localization of PCNA overlaps with that of UCH-L1 in monkey testis (Tokunaga et al., 1999). Our recent study showed that mice lacking UCH-L1 have significantly decreased numbers of PCNA-positive cells in seminiferous tubules (Kwon et al., 2003). These results led us to hypothesize that UCH-L1 may be closely associated with spermatogonial proliferation activity, possibly to maintain the primordial nature of these cells. We thus immunostained testes for PCNA

and UCH-L1. In non-Tg and *gad* testes, PCNA-positive staining was confined to spermatogonia and primary spermatocytes and was not evident in Sertoli cells (Fig. 4A,D,B,E) Similarly, the percentage of PCNA-positive spermatogonia and spermatocytes in the seminiferous tubules of *gad* mice was significantly lower than that of non-Tg mice (Fig. 4A,D,B,E) as we previously observed (Kwon et al., 2003). In contrast, Tg mouse testes showed greater PCNA staining in these cells; surprisingly however, staining was observed in nearly all arrested primary spermatocytes but not in spermatogonia (Fig. 4F). These findings suggest that UCH-L1 plays a specific role in mitotic proliferation. To further clarify the effect of UCH-L1 on PCNA levels, FLAG-tagged *Uchl1* was transfected into GC-1, a germ cell line derived from type B spermatogonia (Hofmann et al., 1992). UCH-L1 (anti-FLAG, Fig. 4G,I, green) and PCNA (Fig. 4H,I, red) were then visualized using immunofluorescence microscopy. Cells transfected with *Uchl1* showed lower PCNA immunoreactivity compared with mock-transfected cells (Fig. 4G), consistent with the assertion that PCNA is downregulated by UCH-L1 in vivo. However, no change of PCNA level was observed in *Uchl3* transfected cells (data not shown),

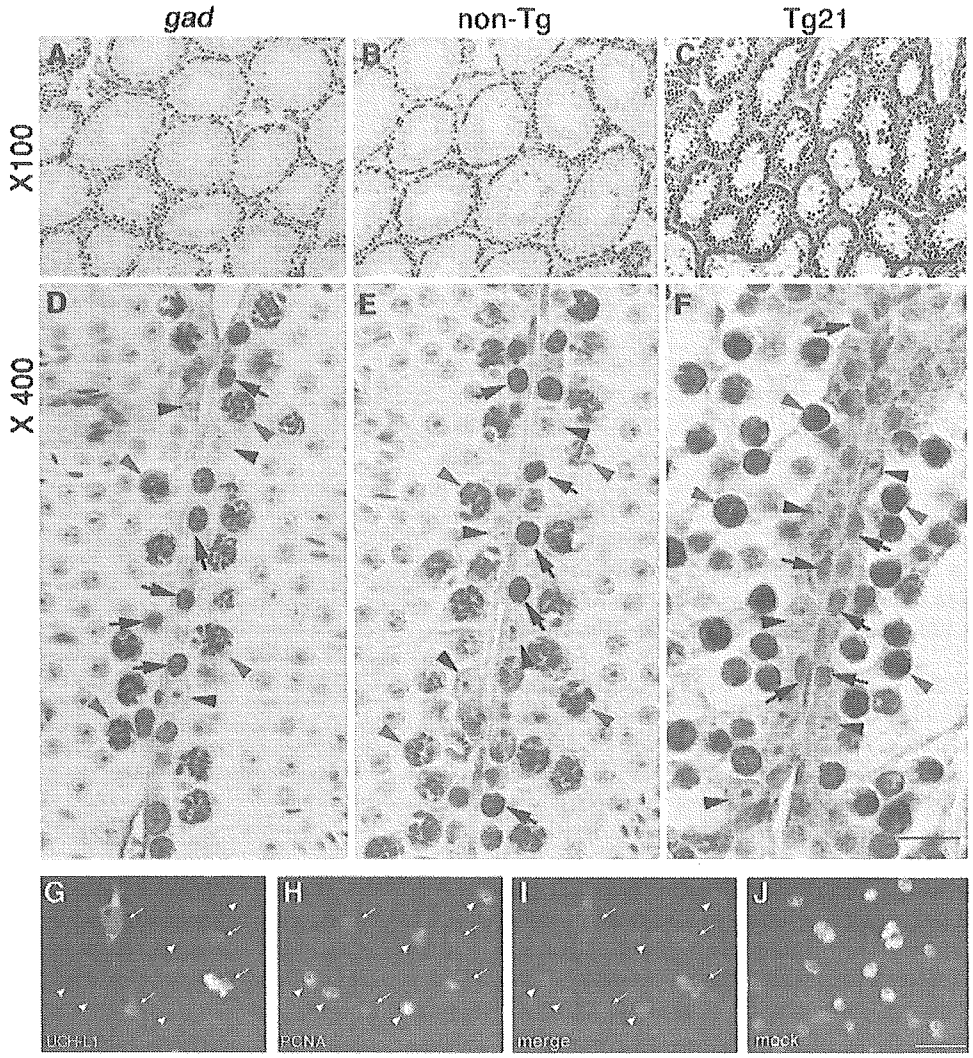

Fig. 4. PCNA immunostaining in the testes of a *gad* mouse (**A**, **D**), a non-Tg mouse (**B**, **E**), a Tg mouse (**C**, **F**; Tg21), and in the transient transfection assay with UCH-L1 using GC-1 cells (**G–J**). In *gad* and non-Tg testes, positive immunostaining was confined to spermatogonia (D, E; black arrows) and primary spermatocytes (D, E; red arrowheads), and staining was not seen in Sertoli cells (D, E; black arrowheads). In contrast, cell staining was more intense in the testis of Tg mice; however, this intensity was observed in almost all arrested primary spermatocytes (F; red arrowheads) but not in spermatogonia (F; black arrows). The staining of non-Tg and *gad* mice was essentially identical. However, nearly all the primary spermatocytes from Tg mice had relatively strong reactivity compared with spermatogonia that had very faint PCNA reactivity (black arrows). Plasmid pCIneo-*Uchl1* (G–I) or vector alone (J, mock) was transfected into GC-1 cells and expressed. Antibodies against FLAG (Sigma, monoclonal) and PCNA (BD Transduction Laboratory, polyclonal) were used to detect exogenously expressed UCH-L1 (G, I, green) and endogenous PCNA (H, J, I, red), respectively. Cells expressing a high level of UCH-L1 (G, white arrows) had a relative low level of PCNA (H, white arrows), whereas cells expressing a low level of UCH-L1 (H, white arrowheads) had high PCNA levels (H, white arrowheads). Magnification: (A–C) ×100; (D–J) ×400. Scale bar: **Upper panels** (see **panel C**), 200 μm; **middle panels** (see **panel F**), 50 μm; **lower panels** (see **panel J**), 50 μm.

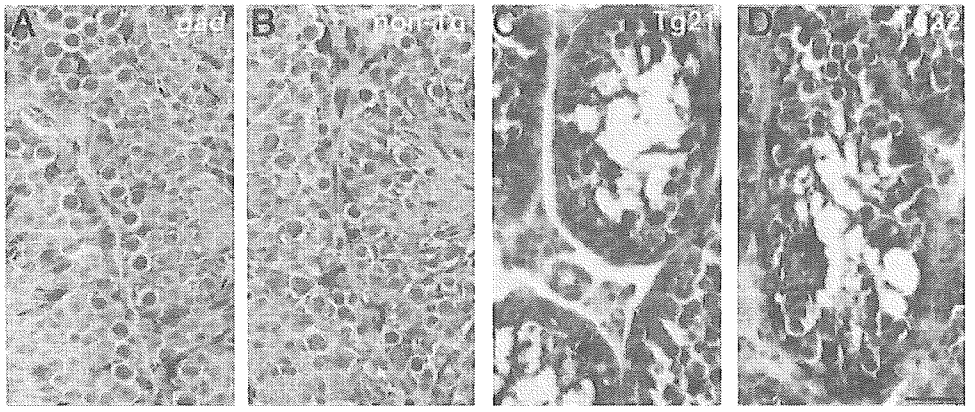

Fig. 5. Vimentin immunostaining in the testes of a *gad* mouse (**A**), a non-Tg mouse (**B**), and Tg mice (**C**, Tg21; **D**, Tg22). No difference was observed in the pattern and density of vimentin staining in Sertoli cells between *gad* (A) and non-Tg testes (B). In contrast, Sertoli cell staining was more intense in the Tg mice (C, D). Magnification: ×400. Scale bar, 200 μm.

suggesting the specificity of UCH-L1 effect on PCNA levels.

Sertoli Cells Exhibit High-Level Vimentin Expression in Tg Mice

We examined the immunoreactivity to vimentin, which is a marker of Sertoli cells (Oke and Suarez-Quian, 1993; Mori et al., 1997). Vimentin immunostaining was observed in Sertoli cells, and there is no difference between *gad* and non-Tg mice (Fig. 5A,B). In contrast, very strong expression of vimentin was observed in almost all Sertoli cells throughout the cytoplasm in Tg mice (Fig. 5C,D).

Bcl-2 Downregulation and Caspase-3 Upregulation in Tg Mice

The two key proteins, Bcl-2 and caspases-3 that involved in testicular germ cell apoptosis are especially altered during spermatogenesis or stress-induced germ cell apoptosis in *gad*mice (Harada et al., 2004; Kwon et al., 2004b, 2005). We thus examined the expression of these proteins in Tg and non-Tg testes to determine whether they are actually involved in countering increased apoptosis. Bcl-2 expression was downregulated in the testes of Tg mice compared with non-Tg mice (Fig. 6). In contrast to non-Tg mice, Tg mice had an elevated level of the activated caspase-3 subunit, p17 (Fig. 6), controversial to that observed in the retina of *gad* mice after ischemic injury (Harada et al., 2004). These results are consistent with the profound difference in UCH-L1 expression in these two mouse lines.

Upregulations of both Mono- and Poly-Ubiquitin in Tg Mice

Our recent studies suggested novel functions for UCH-L1, namely that it effectively upregulates ubiquitin levels at the post-transcriptional level (Osaka et al., 2003) and that ubiquitin induction plays a critical role in regulating cell death during cryptorchid injury–mediated germ cell apoptosis (Kwon et al., 2004b). Moreover, the testes of mice expressing K48R mutant ubiquitin are protected from cryptorchid injury (Rasoulpour et al., 2003). Given this information, we examined ubiquitin levels in *Uchl1* Tg mice. As expected, ubiquitin expression was strong in testicular cells of Tg mice (Fig. 7C,D), particularly in the arrested spermatocytes, but its expression was low in *gad* mice (Fig. 7B) compared with non-Tg mice (Fig. 7A). These data provide additional evidence that ubiquitin expression is induced upon UCH-L1 overexpression. To determine whether the increased ubiquitin staining represented monoubiquitin or polyubiquitin, we next examined the levels of both ubiquitin forms via immunoblotting (Fig. 7E). As expected, mono- and poly-ubiquitin levels in Tg mice were substantially higher than in non-Tg mice. A *gad* mouse control had relatively low levels

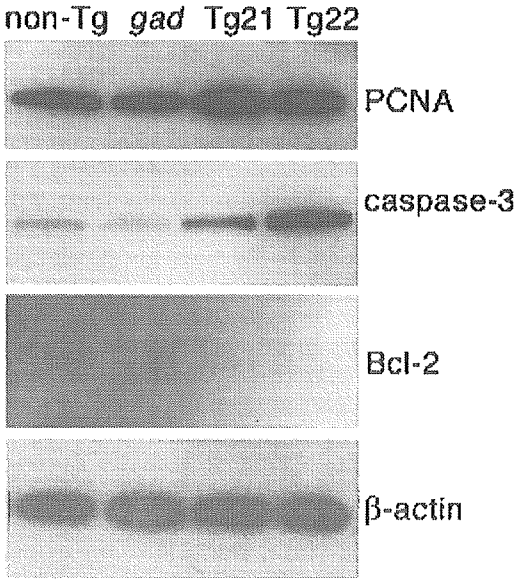

Fig. 6. Western blot analysis of Tg mouse testicular lysates. Consistent with the immunohistochemistry results, PCNA and caspase-3 substantially accumulated in Tg mice. However, the expression of antiapoptotic Bcl-2 decreased compared with non-Tg or *gad* mice.

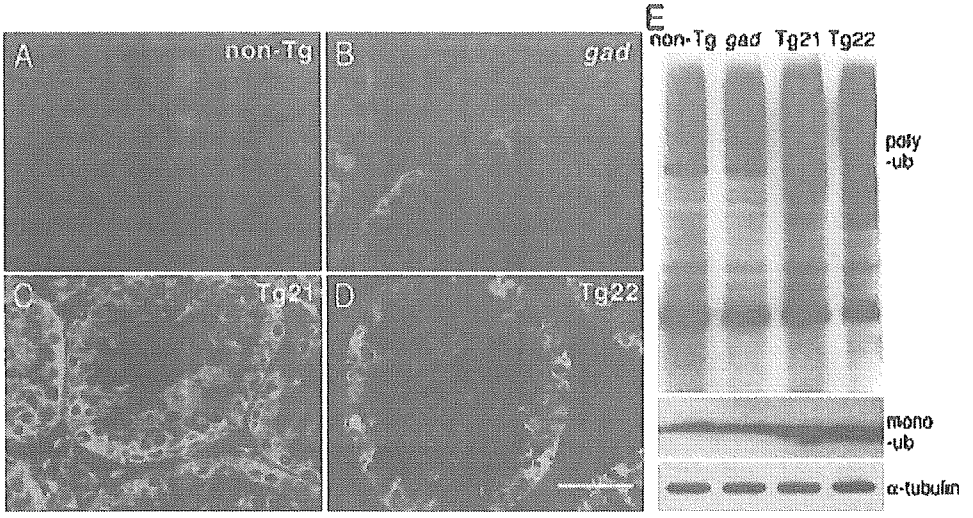

Fig. 7. The levels of mono- and poly-ubiquitin in the testes of non-Tg and Tg males. Double immunostaining for UCH-L1 and ubiquitin in the testis (**A**, non-Tg; **B**, *gad*; **C**, Tg21; **D**, Tg22). All strongly UCH-L1-positive cells (green) were also strongly positive for ubiquitin (red) in the two male Tg mice. Scale bar, 50 μm. **E.** An immunoblot showing that both mono- and poly-ubiquitin expression were significantly increased in the two Tg mice compared with non-Tg and *gad* mice (ub, ubiquitin).

of both mono- and poly-ubiquitin (Fig. 7E). These findings are consistent with previous studies and support the hypothesis that UCH-L1-mediated spermatocyte apoptosis involves the induction of ubiquitin expression.

DISCUSSION

Apoptosis in testicular germ cells is regulated by a complicated signal transduction pathway; however, the molecular mechanisms regulating this process are uncertain. We recently showed that *gad* mice, lacking UCH-L1 function, are resistant to apoptotic stress (Harada et al., 2004; Kwon et al., 2004b). These observations conclusively indicate that UCH-L1 plays a role in germ cell death during experimental stress-induced apoptosis. We thus hypothesized that germ cell apoptosis is directly induced by excess UCH-L1. To test this hypothesis, we utilized three mouse lines, wild-type (non-Tg), *gad* and *Uchl1* Tgs, which differ with respect to UCH-L1 expression. In Tg mice, germ cell apoptosis was barely detectable in spermatogonia or Sertoli cells, both of which strongly expressed UCH-L1. Apoptosis was observed mainly in primary spermatocytes, which had weak or negative UCH-L1 expression although they are derived from spermatogonia. These data suggest that excess UCH-L1 in fact does not directly induce apoptosis in spermatogonia or somatic Sertoli cells. These data further provoke the question of why apoptosis occurs during spermatocyte meiosis.

In our *Uchl1* Tg mice, there was no evidence of spermatogonia or Sertoli cell apoptosis despite the fact that these cells had stronger UCH-L1 expression compared with non-Tg mice. Accordingly, it could be concluded that overexpression of UCH-L1 in spermatogonia does not directly induce apoptosis in these cells (nor in Sertoli cells). Because spermatocytes are genetically distinct from the original mother cell (spermatogonia), we speculate that the Tg mice are highly susceptible to spermatocyte apoptosis in vivo, with the inference that spermatocytes seem to be particularly sensitive to UCH-L1 overexpression in spermatogonia even though spermatocytes themselves express a much lower level of UCH-L1. In contrast, *gad* mice are resistant to cryptorchid-induced germ cell apoptosis, and many germ cells undergo apoptosis in older animals although their testes develop nearly normally and produce mature sperm (Kwon et al., 2004b). These data suggest that the lack of UCH-L1 causes mice to have lower sensitivity to stress compared with wild-type males, although UCH-L1 is probably not essential for spermatogenesis under normal conditions. On one hand, UCH-L1 seems to be necessary for the stabilization of germ cells to protect against aging-associated apoptosis; however, the stabilization of germ cells appears to be limited by the concentration of UCH-L1, and consequently they may be damaged during spermatocyte meiosis when UCH-L1 is overexpressed. Despite the fact that excess UCH-L1 does not induce spermatogonial apoptosis, abnormalities in intracellular regulatory factors may potentially influence mitosis directly (i.e., as the cell divides into two daughter cells—spermatocytes). Some of these factors may accumulate or be reduced in the presence of excess UCH-L1, thereby causing disruptions such as arrested meiosis or the onset of apoptosis in spermatocytes rather than spermatogonia (Fig. 8).

Many of the factors involved in cellular apoptosis, including the Bcl-2 family and caspases, are targets for ubiquitynation. Previously, we have shown that Bcl-2 is upregulated (Kwon et al., 2004b) and caspases-3 is downregulated (Kwon et al., 2005) in *gad* mice. The decreased level of Bcl-2 and increased level of caspases-3

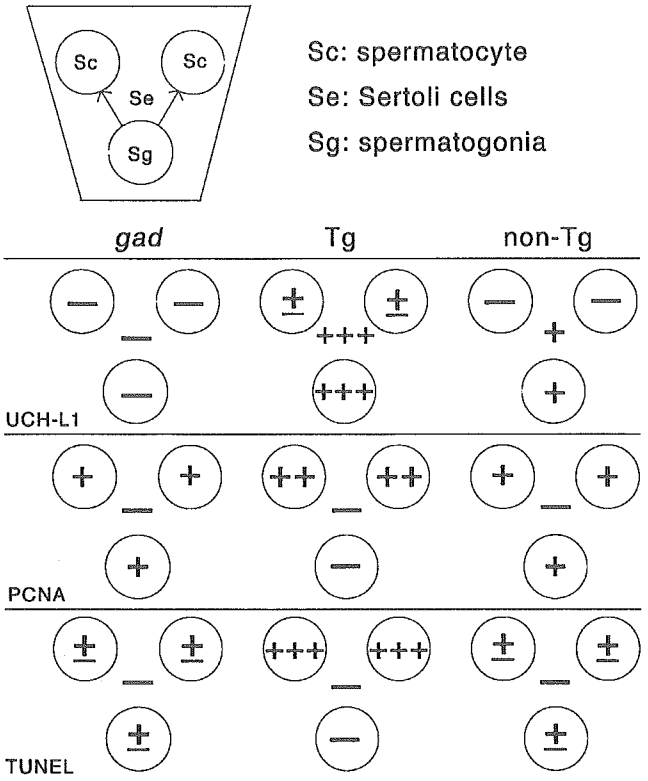

Fig. 8. TUNEL activity, and UCH-L1 and PCNA immunoreactivities in seminiferous tubules of non-Tg, *gad* and Tg mice. TUNEL activity or immunoreactivity: +++, strong; ++, moderate; + to ±, low to weak; −, not detectable.

observed in Tg mice in this study suggest that UCH-L1 can regulates the apoptosis during spermatogenesis by influencing the balance between apoptotic and anti-apoptotic proteins.

PCNA is ubiquitylated at lysine 48 (K48) and degraded by the ubiquitin-proteasome system (Yamamoto et al., 2004). In addition, PCNA is also monoubiquitylated at K164, thereby priming K63-linked polyubiquitin chains, which unlike K48-linked chains, do not promote proteasomal degradation (Hoege et al., 2002). In our present study, excess UCH-L1 relocalized PCNA from spermatogonia to spermatocytes and Sertoli cells in vivo and reduced PCNA expression to a low level in vitro. Based on these data, we hypothesize that UCH-L1, at least in part, may influence germ cell meiosis by affecting PCNA ubiquitynation, thereby disrupting its localization. In fact, PCNA significantly accumulated in primary spermatocytes of Tg mice (Fig. 4F). Since we did not obtain data regarding PCNA ubiquitylation in Tg mice, it is not clear whether the accumulated PCNA we observed was monoubiquitylated or polyubiquitylated. In any case, the accumulation of PCNA in primary spermatocytes may alter, damage or interrupt physical functions during meiosis (Fig. 8).

Germ cells and Sertoli cells are the only cell types expressed inside seminiferous tubules (McLaren, 1998). Germ cells constitute the male meiotic contribution to the reproductive cycle, whereas Sertoli cells support the growth and differentiation of germ cells. Direct interaction between germ cells and Sertoli cells may constitute an important part of the regulation of spermatogenesis (Russell et al., 1993). Indeed, mice exposed to Sertoli cell toxicants exhibit increased germ cell apoptosis (Lee et al., 1999). Therefore, Sertoli cells play a special role in nurturing and controlling spermatogenesis. Until postnatal day 16, UCH-L1 localizes only to spermatogonia, whereas after day 30 it also appears in Sertoli cells (Kon et al., 1999). Therefore, although UCH-L1 is highly expressed in both spermatogonia and somatic Sertoli cells, its function may be cell type-dependent. Under normal conditions UCH-L1 is a marker for activated Sertoli cells, in which it plays an important role in the degradation of abnormal proteins via the ubiquitin-proteasome system (Kon et al., 1999). Thus, we suspect that germ cell apoptosis in Tg mice might be related to the abnormal physical conditions in these cells. Our present work demonstrates that Tg mouse Sertoli cells are intensely immunoreactivity for UCH-L1, as expected. Furthermore, with vimentin, which is a marker present only in Sertoli cells (Oke and Suarez-Quian, 1993; Mori et al., 1997), we showed in this study that Tg mice had more vimentin immunoreactivity than non-Tg or *gad* mice (Fig. 5). Thus, forced expression of UCH-L1 in Sertoli cells perhaps may lead to gain of UCH function, thereby interrupting Sertoli cell-germ cell interactions that in turn promote germ cell apoptosis (Fig. 8).

In conclusion, we have demonstrated that UCH-L1 is an important spermatogenic factor related to PCNA and ubiquitin function. We used Tg mice overexpressing UCH-L1 to identify a new role for this protein. Overexpression of the *Uchl1* transgene inhibited spermatogenesis and induced germ cell death via an apoptotic mechanism, leading to male sterility. To our knowledge, the present data constitute the first description of a proapoptotic role for UCH-L1 in *Uchl1* Tg mice, as clearly revealed by the morphological and TUNEL results. Although UCH-L1 is constitutively expressed during spermatogenesis, and spermatogenic cell apoptosis is a normal aspect of mammalian spermatogenesis (Allan et al., 1992; Furuchi et al., 1996), the frequent cell death found in our *Uchl1* Tg mice could reflect an exaggeration of naturally occurring apoptosis. However, at present we do not understand whether the *Uchl1* transgene acts solely by inducing apoptosis or by interfering with differentiation so as to cause germ cell loss. This issue must be addressed to more fully define the role of UCH-L1 in the regulation and fate of spermatogonia during spermatogenesis.

ACKNOWLEDGMENTS

We thank H. Kikuchi for assistance in preparing the sections and M. Shikama for the care and breeding of animals.

REFERENCES

Allan DJ, Harmon BV, Roberts SA. 1992. Spermatogonial apoptosis has three morphologically recognizable phases and shows no circadian

rhythm during normal spermatogenesis in the rat. Cell Prolif 25: 241–250.

Aoki S, Su Q, Li H, Nishikawa K, Ayukawa K, Hara Y, Namikawa K, Kiryu-Seo S, Kiyama H, Wada K. 2002. Identification of an axotomy-induced glycosylated protein, AIGP1, possibly involved in cell death triggered by endoplasmic reticulum-Golgi stress. J Neurosci 22: 10751–10760.

Baarends WM, van der Laan R, Grootegoed JA. 2000. Specific aspects of the ubiquitin system in spermatogenesis. J Endocrinol Invest 23: 597–604.

Furuchi T, Masuko K, Nishimune Y, Obinata M, Matsui Y. 1996. Inhibition of testicular germ cell apoptosis and differentiation in mice misexpressing Bcl-2 in spermatogonia. Development 122: 1703–1709.

Harada T, Harada C, Wang YL, Osaka H, Amanai K, Tanaka K, Takizawa S, Setsuie R, Sakurai M, Sato Y, Noda M, Wada K. 2004. Role of ubiquitin carboxy terminal hydrolase-L1 in neural cell apoptosis induced by ischemic retinal injury in vivo. Am J Pathol 164:59–64.

Hoege C, Pfander B, Moldovan GL, Pyrowolakis G, Jentsch S. 2002. RAD6-dependent DNA repair is linked to modification of PCNA by ubiquitin and SUMO. Nature 419:135–141.

Hofmann MC, Narisawa S, Hess RA, Millan JL. 1992. Immortalization of germ cells and somatic testicular cells using the SV40 large T antigen. Exp Cell Res 201:417–435.

Imai T, Kawai Y, Tadokoro Y, Yamamoto M, Nishimune Y, Yomogida K. 2004. In vivo and in vitro constant expression of GATA-4 in mouse postnatal Sertoli cells. Mol Cell Endocrinol 214:107–115.

Kelman Z. 1997. PCNA: Structure, functions, and interactions. Oncogene 14:629–640.

Kon Y, Endoh D, Iwanaga T. 1999. Expression of protein gene product 9.5, a neuronal ubiquitin C-terminal hydrolase, and its developing change in sertoli cells of mouse testis. Mol Reprod Dev 54:333–341.

Kroll KL, Amaya E. 1996. Transgenic *Xenopus* embryos from sperm nuclear transplantations reveal FGF signaling requirements during gastrulation. Development 122:3173–3183.

Kurihara LJ, Kikuchi T, Wada K, Tilghman SM. 2001. Loss of Uch-L1 and Uch-L3 leads to neurodegeneration, posterior paralysis, and dysphagia. Hum Mol Genet 10:1963–1970.

Kwon J, Kikuchi T, Setsuie R, Ishii Y, Kyuwa S, Yoshikawa Y. 2003. Characterization of the testis in congenitally ubiquitin carboxy-terminal hydrolase-1 (Uch-L1) defective (gad) mice. Exp Anim 52: 1–9.

Kwon J, Wang YL, Setsuie R, Sekiguchi S, Sakurai M, Sato Y, Lee WW, Ishii Y, Kyuwa S, Noda M, Wada K, Yoshikawa Y. 2004a. Developmental regulation of ubiquitin C-terminal hydrolase isozyme expression during spermatogenesis in mice. Biol Reprod 71: 515–521.

Kwon J, Wang YL, Setsuie R, Sekiguchi S, Sato Y, Sakurai M, Noda M, Aoki S, Yoshikawa Y, Wada K. 2004b. Two closely related ubiquitin C-terminal hydrolase isozymes function as reciprocal modulators of germ cell apoptosis in cryptorchid testis. Am J Pathol 165:1367–1374.

Kwon J, Mochida K, Wang YL, Sekiguchi S, Sankai T, Aoki S, Ogura A, Yoshikawa Y, Wada K. 2005. Ubiquitin C-terminal hydrolase L-1 is essential for the early apoptotic wave of germinal cells and for sperm quality control during spermatogenesis. Biol Reprod 73:29–35.

Lee J, Richburg JH, Shipp EB, Meistrich ML, Boekelheide K. 1999. The Fas system: A regulator of testicular germ cell apoptosis, is differentially up-regulated in Sertoli cell versus germ cell injury of the testis. Endocrinology 140:852–858.

Matzuk MM, Lamb DJ. 2002. Genetic dissection of mammalian fertility pathways. Nat Cell Biol 4:s41–s49.

McLaren A. 1998. Gonad development: Assembling the mammalian testis. Curr Biol 8:R175–R177.

Mizushima S, Nagata S. 1990. pEF-BOS: A powerful mammalian expression vector. Nucleic Acids Res 18:5322.

Mori C, Nakamura N, Dix DJ, Fujioka M, Nakagawa S, Shiota K, Eddy EM. 1997. Morphological analysis of germ cell apoptosis during postnatal testis development in normal and Hsp 70-2 knockout mice. Dev Dyn 208:125–136.

Oke BO, Suarez-Quian CA. 1993. Localization of secretory, membrane-associated, and cytoskeletal proteins in rat testis using an improved immunocytochemical protocol that employs polyester wax. Biol Reprod 48:621–631.

Osaka H, Wang YL, Takada K, Takizawa S, Setsuie R, Li H, Sato Y, Nishikawa K, Sun YJ, Sakurai M, Harada T, Hara Y, Kimura I, Chiba S, Namikawa K, Kiyama H, Noda M, Aoki S, Wada K. 2003. Ubiquitin carboxy-terminal hydrolase L1 binds to and stabilizes monoubiquitin in neuron. Hum Mol Genet 12:1945–1958.

Osawa Y, Wang YL, Osaka H, Aoki S, Wada K. 2001. Cloning, expression, and mapping of a mouse gene, *Uchl4*, highly homologous to human and mouse Uchl3. Biochem Biophys Res Commun 283: 627–633.

Rasoulpour RJ, Schoenfeld HA, Gray DA, Boekelheide K. 2003. Expression of a K48R mutant ubiquitin protects mouse testis from cryptorchid injury and aging. Am J Pathol 163:2595–2603.

Russell LD, Corbin TJ, Borg KE, De Franca LR, Grasso P, Bartke A. 1993. Recombinant human follicle-stimulating hormone is capable of exerting a biological effect in the adult hypophysectomized rat by reducing the numbers of degenerating germ cells. Endocrinology 133:2062–2070.

Saigoh K, Wang YL, Suh JG, Yamanishi T, Sakai Y, Kiyosawa H, Harada T, Ichihara N, Wakana S, Kikuchi T, Wada K. 1999. Intragenic deletion in the gene encoding ubiquitin carboxy-terminal hydrolase in gad mice. Nat Genet 23:47–51.

Sutovsky P. 2003. Ubiquitin-dependent proteolysis in mammalian spermatogenesis, fertilization, and sperm quality control: Killing three birds with one stone. Microsc Res Tech 61:88–102.

Tokunaga Y, Imai S, Torii R, Maeda T. 1999. Cytoplasmic liberation of protein gene product 9.5 during the seasonal regulation of spermatogenesis in the monkey (*Macaca fuscata*). Endocrinology 140:1875–1883.

Toschi L, Bravo R. 1988. Changes in cyclin/proliferating cell nuclear antigen distribution during DNA repair synthesis. J Cell Biol 107: 1623–1628.

Wilkinson KD. 2000. Ubiquitination and deubiquitination: Targeting of proteins for degradation by the proteasome. Semin Cell Dev Biol 11:141–148.

Williams K, Schwartz A, Corey S, Orandle M, Kennedy W, Thompson B, Alvarez X, Brown C, Gartner S, Lackner A. 2002. Proliferating cellular nuclear antigen expression as a marker of perivascular macrophages in simian immunodeficiency virus encephalitis. Am J Pathol 161:575–585.

Wing SS. 2003. Deubiquitinating enzymes—the importance of driving in reverse along the ubiquitin-proteasome pathway. Int J Biochem Cell Biol 35:590–605.

Yamamoto T, Kimura S, Mori Y, Oka M, Ishibashi T, Yanagawa Y, Nara T, Nakagawa H, Hashimoto J, Sakaguchi K. 2004. Degradation of proliferating cell nuclear antigen by 26S proteasome in rice (*Oryza sativa* L.). Planta 218:640–646.

Yamazaki K, Wakasugi N, Tomita T, Kikuchi T, Mukoyama M, Ando K. 1988. Gracile axonal dystrophy (GAD): A new neurological mutant in the mouse. Proc Soc Exp Biol Med 187:209–215.

Yuan L, Liu JG, Zhao J, Brundell E, Daneholt B, Hoog C. 2000. The murine *SCP3* gene is required for synaptonemal complex assembly, chromosome synapsis, and male fertility. Mol Cell 5:73–83.

BIOLOGY OF REPRODUCTION 73, 29–35 (2005)
Published online before print 2 March 2005.
DOI 10.1095/biolreprod.104.037077

Ubiquitin C-Terminal Hydrolase L-1 Is Essential for the Early Apoptotic Wave of Germinal Cells and for Sperm Quality Control During Spermatogenesis[1]

Jungkee Kwon,[3,4] Keiji Mochida,[5] Yu-Lai Wang,[3] Satoshi Sekiguchi,[4] Tadashi Sankai,[6] Shunsuke Aoki,[3] Atsuo Ogura,[5] Yasuhiro Yoshikawa,[4] and Keiji Wada[2,3]

Department of Degenerative Neurological Disease,[3] National Institute of Neuroscience, National Center of Neurology and Psychiatry, Kodaira, Tokyo 187-8502, Japan
Department of Biomedical Science,[4] Graduate School of Agricultural and Life Sciences, University of Tokyo, Bunkyo-ku, Tokyo 113-8657, Japan
Bioresource Engineering Division,[5] Bioresource Center, Riken, Tsukuba, Ibaraki 305-0074, Japan
Tsukuba Primate Center,[6] National Institute of Infectious Diseases, Tsukuba, Ibaraki 305-0843, Japan

ABSTRACT

Ubiquitination is required throughout all developmental stages of mammalian spermatogenesis. Ubiquitin C-terminal hydrolase (UCH) L1 is thought to associate with monoubiquitin to control ubiquitin levels. Previously, we found that UCHL1-deficient testes of *gad* mice have reduced ubiquitin levels and are resistant to cryptorchid stress-related injury. Here, we analyzed the function of UCHL1 during the first round of spermatogenesis and during sperm maturation, both of which are known to require ubiquitin-mediated proteolysis. Testicular germ cells in the immature testes of *gad* mice were resistant to the early apoptotic wave that occurs during the first round of spermatogenesis. TUNEL staining and cell quantitation demonstrated decreased germ cell apoptosis and increased numbers of premeiotic germ cells in *gad* mice between Postnatal Days 7 and 14. Expression of the apoptotic proteins TRP53, Bax, and caspase-3 was also significantly lower in the immature testes of *gad* mice. In adult *gad* mice, cauda epididymidis weight, sperm number in the epididymis, and sperm motility were reduced. Moreover, the number of defective spermatozoa was significantly increased; however, complete infertility was not detected. These data indicate that UCHL1 is required for normal spermatogenesis and sperm quality control and demonstrate the importance of UCHL1-dependent apoptosis in spermatogonial cell and sperm maturation.

apoptosis, early apoptotic wave, epididymis, gad *mouse, sperm, spermatogenesis, sperm quality, testis, UCHL1*

INTRODUCTION

Ubiquitin and ubiquitin-dependent proteolysis are involved in a variety of cellular processes, such as cell cycle progression, degradation of intracellular proteins, programmed cell death, and membrane receptor endocytosis [1–5]. In spermatogenesis, the ubiquitin-proteasome system is required for the degradation of numerous proteins throughout the mitotic, meiotic, and postmeiotic developmental phases [4, 6, 7]. Ubiquitin C-terminal hydrolases (UCHs) control the cellular ubiquitin balance by releasing ubiquitin from tandemly conjugated ubiquitin monomers (*Ubb, Ubc*) and small adducts or unfolded polypeptides [4, 8–10]. UCHL1 is expressed at high levels in both testis and epididymis and may play an important role in the regulation of spermatogenesis [11–14]. In addition to its hydrolase activity [15], UCHL1 has a variety of functions, including dimerization-dependent ubiquityl ligase activity, and association with and stabilization of monoubiquitin in neuronal cells [16–18]. Furthermore, it has been suggested that UCHL1 also functions as a regulator of apoptosis [19]. The gracile axonal dystrophy (*gad*) mouse is an autosomal recessive spontaneous mutant carrying an intragenic deletion of the gene encoding *Uchl1* [21]. We recently found that testes of *gad* mice, which lack UCHL1 expression [18, 20, 21], have reduced ubiquitin levels and are resistant to cryptorchid injury-mediated germ cell apoptosis [22].

During prepubertal development, an early and massive wave of germinal cell apoptosis occurs in mouse testis [23, 24]. This early germ cell apoptotic wave affects mainly spermatogonia and spermatocytes and appears to be essential for functional spermatogenesis in adulthood. Decreased apoptosis has been reported in the early phase of spermatogenesis in transgenic mice overexpressing the antiapoptotic proteins *Bcl2* or *Bcl-xL* [23, 25] and in mice deficient in the apoptotic protein *Bax* [26]. This reduction in apoptosis is associated with the disruption of normal spermatogenesis and infertility. Our previous work demonstrated that *gad* mice exhibit pathological changes such as progressively decreasing spermatogonial stem cell proliferation [13] and increased expression of the antiapoptotic proteins Bcl2 and Bcl-xL in response to apoptotic stress [19, 22]. Furthermore, we showed that UCHL1 functions during prepubertal development to effect normal spermatogenesis and to modulates germ cell apoptosis [22]. However, the mechanism by which UCHL1 regulates apoptosis during prepubertal development remains unclear. To further investigate the role of UCHL1 in immature testes, we evaluated the function of UCHL1 during early spermatogenesis. Here, we show that immature testes of *gad* mice accumulate premeiotic germ cells and are resistant to the massive wave of germinal cell apoptosis during the first round of spermatogenesis, eventually leading to alterations in sperm produc-

[1]Supported by Grants-in-Aid for Scientific Research from the Ministry of Health, Labour and Welfare of Japan; Grants-in-Aid for Scientific Research from the Ministry of Education, Culture, Sports, Science and Technology of Japan; a grant from the Pharmaceuticals and Medical Devices Agency of Japan; and a grant from Japan Science and Technology Agency.
[2]Correspondence: Keiji Wada, Department of Degenerative Neurological Disease, National Institute of Neuroscience, National Center of Neurology and Psychiatry, Kodaira, Tokyo 187-8502, Japan.
FAX: 81 42 341 1745; e-mail: wada@ncnp.go.jp

Received: 16 October 2004.
First decision: 16 December 2004.
Accepted: 21 February 2005.

ISSN: 0006-3363. http://www.biolreprod.org

tion, motility, and morphology in adult mice. Our data suggest that UCHL1-dependent apoptosis is essential for normal spermatogenesis.

MATERIALS AND METHODS

Animals

We used male *gad* (CBA/RFM) mice [21] at 7, 14, 21, 28, and 35 days and 10 wk of age. The *gad* mouse is an autosomal-recessive mutant that was produced by crossing CBA and RFM mice. The *gad* line was maintained by intercrossing for more than 20 generations. This strain was maintained at our institute. Animal care and handling were in accordance with institutional regulations and were approved by the Animal Investigation Committee of the National Institute of Neuroscience, National Center of Neurology and Psychiatry.

Histological and Immunohistochemical Assessment of Testes

Testes were embedded in paraffin wax after fixation in 4% paraformaldehyde, sectioned at 4-μm thickness, and stained with hematoxylin for counting [13]. Light microscopy was used for routine observations. For immunohistochemical staining, the sections were incubated with 10% goat serum for 1 h at room temperature followed by incubation overnight at 4°C with a rabbit polyclonal antibody against UCHL1 (1:1000 dilution; peptide antibody) [20] in PBS containing 1% BSA. Sections were then incubated for 1 h with biotin-conjugated anti-rabbit IgG diluted 1:200 in PBS, followed by Vectorstain ABC-PO (Vector Laboratories, Burlingame, CA) for 30 min at room temperature. Sections were developed using 3,3′-diaminobenzidine and counterstained with hematoxylin.

Apoptotic cells in testicular tissues were identified by terminal deoxynucleotidyl transferase (TdT)-mediated nick end labeling (TUNEL) using the DeadEnd Fluorometric TUNEL system (Promega, Madison, WI) according to the manufacturer's instructions.

Quantitative Analysis of Testicular Cell Number

The total number of cells was determined by counting the testicular cells including Sertoli cells of seminiferous tubules. Quantitative determinations were made using four each of wild-type and *gad* mice at 7 and 14 days of age. Five sections from each mouse were processed in parallel for counterstaining with hematoxylin. Twenty circular seminiferous tubules in each section were then selected by randomly from those tubules, and 400 circular seminiferous tubules were measured using the 400× lens of a Zeiss Axioplan microscope. The total cell number was not determined by dividing cell types such as testicular germ cells and Sertoli cells because it was difficult to determine the difference of cell types [26]. There were no significant differences in nuclear size in either of the group studies. Thus, the total number of cells reflected all cell types of seminiferous tubules.

Quantitative Analysis of Apoptotic Germ Cells

Quantification was performed using four each of wild-type and *gad* mice at 7, 14, 21, 28, and 35 days of age. The total number of apoptotic cells was determined by counting the positively stained nuclei in 20 circular seminiferous tubules in each section [22]. Five sections from each mouse and a total 400 circular seminiferous tubules per each group were processed.

Germ Cell Isolation, Culture, and Viability Measurement

Germ cells from wild-type and *gad* mice were prepared using a modification of the procedure described by Kwon et al. [20]. Briefly, testes from three 2-wk-old mice were incubated twice for 30 min at 25°C in Dulbecco Modified Eagle medium (DMEM)-F12 medium containing 0.5 mg/ml collagenase IV-S (Sigma-Aldrich, St. Louis, MO) and then digested for 60 min at 25°C in DMEM-F12 medium containing 1 mg/ml trypsin (Sigma-Aldrich). The cell suspension was digested and washed several times to eliminate testicular somatic cells. The cells were then counted and cultured at 2.0×10^5 cells/ml in DMEM-F12 medium containing 10% fetal bovine serum (FBS). The cells were harvested at each day for 5 days, and viability was assessed using the Vi-Cell XR cell viability analyzer (Beckman Coulter, Fullerton, CA).

Quantitative mRNA Analysis of Uchl1 and Uchl3 Genes by Real-Time PCR

SYBR Green-based real-time quantitative reverse transcription-polymerase chain reaction (RT-PCR; PRISM 7700 Sequence detection system, ABI, Columbia, MD) was performed [20] in SYBR Green Master mix using the following primers: *Uchl1*, 5′-TTCTGTTCAACAACGTGGAC G-3′ and 5′-TCACTGGAAAGGGCATTCG-3′; *Uchl3*, 5′-TGAAGGTC AGACTGAGGCACC-3′ and 5′-AATTGGAAATGGTTTCCGTCC-3′; β-actin, 5′-CGTGCGTGACATCAAAGAGAA-3′ and 5′-CAATAGTGAT-GACCTGGCCGT-3′ To compare *Uchl1* and *Uchl3* gene expression in the first round of spermatogenesis, the formula 2^{-ddCt} was used to calculate relative expression compared with testes of 7-day-old mice.

Western Blotting

Western blots were performed as previously reported [19, 22]. Total protein (5 μg/lane) was subjected to SDS-polyacrylamide gel electrophoresis using 15% gels (Perfect NT Gel, DRC, Japan). Proteins were electrophoretically transferred to polyvinylidene difluoride membranes (Bio-Rad, Hercules, CA) and blocked with 5% nonfat milk in TBS-T (50 mM Tris base, pH 7.5, 150 mM NaCl, 0.1% [w/v] Tween-20). The membranes were incubated individually with one or more primary antibodies to UCHL1 and UCHL3 (1:1000 dilution; peptide antibodies) [20], Bcl-xL, Bax, TRP53, and inactive caspase-3 (1:1000 dilution; all from Cell Signaling Technology, Beverly, MA). Blots were further incubated with peroxidase-conjugated goat anti-mouse IgG or goat anti-rabbit IgG (1:5000 dilution; Pierce, Rockford, IL) for 1 h at room temperature. Immunoreactions were visualized using the SuperSignal West Dura Extended Duration Substrate (Pierce) and analyzed using a ChemiImager (Alpha Innotech, San Leandro, CA).

Sperm Motility, Morphology, and Immunohistochemical Assessments

Sperm were collected from the right cauda epididymidis [27] of 10-wk-old wild-type and *gad* mice in 400 μl human tubal fluid medium containing 0.5% bovine serum albumin and then incubated at 37°C under 5% CO_2 in air for 1–2 h. Using a computer-assisted semen analysis system (TOX IVOS, Hamilton Throne Research, Beverly, MA) [28], sperm were analyzed for the following motion parameters: percentage of motile sperm (MSP), percentage of progressively motile sperm (PMP), average path velocity (VAP), straight-line velocity (VSL), curvilinear velocity (VCL), lateral head displacement (ALH), linearity (VSL/VCL × 100), and straightness (VSL/VAP × 100). All procedures were performed at 37°C. To study the spermatozoa morphology, sperm were smeared and then evaluated for defects in the head, midpiece, and principal piece and for head detachment. For immunocytochemical staining, the sections were incubated with antibodies against UCHL1 (1:1000 dilution; peptide antibody) [20] and ubiquitin (1:500 dilution; DakoCytomation, Glostrup, Denmark) overnight at 4°C in PBS containing 1% BSA.

Statistical Analysis

The mean and standard deviation were calculated for all data (presented as mean ± SD). One-way analysis of variance (ANOVA) was used for all statistical analyses.

RESULTS

Expression of UCHL1 During the First Round of Spermatogenesis

We used Western blotting to characterize the level of UCHL1 and UCHL3 expression in testes from immature wild-type and *gad* mice (Fig. 1, B and C). In agreement with previous data [20], UCHL1 expression was significantly elevated on Day 14 in testicular lysates obtained from 7-, 14-, 21-, 28-, and 35-day-old wild-type mice. The level of UCHL3 expression increased with age and did not differ between *gad* and wild-type mice (Fig. 1B), suggesting that UCHL3 expression is regulated independently of UCH-L1 during the first round of spermatogenesis [20]. We also assessed the expression pattern of *Uchl1* and *Uchl3* genes during juvenile spermatogenesis using SYBR Green-

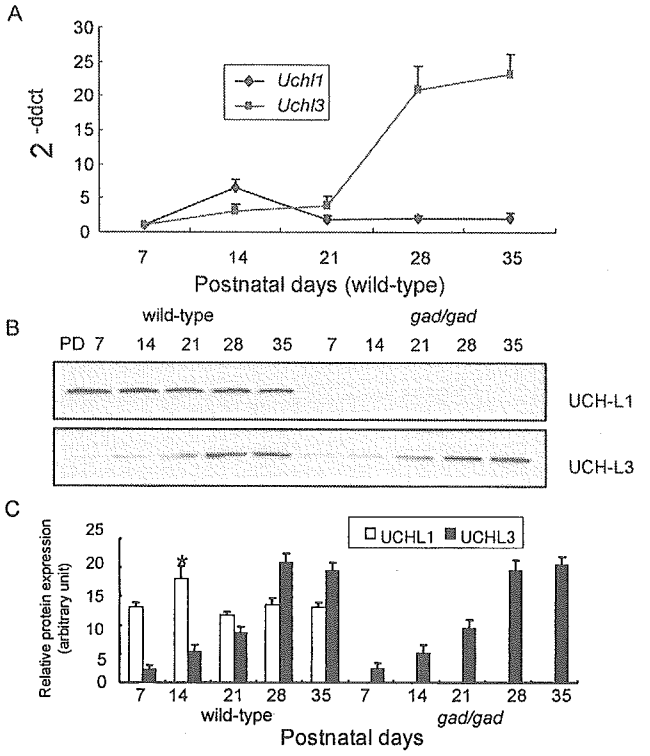

FIG. 1. Expression of UCHL1 and UCHL3during the first round of spermatogenesis. **A)** Comparison of *Uchl1* and *Uchl3* gene expression levels (2^{-ddCt}) by SYBR Green-based real-time quantitative reverse transcription-polymerase chain reaction (RT-PCR). The value for gene expression from the testes of 7-day-old mice was set to 1.0. **B)** Comparison of UCHL1 and UCHL3 expression by Western blotting of testicular lysates from wild-type or *gad* mice. Blots were reprobed for α-tubulin, which was used to normalize the protein load. Representative images from four independent experiments are shown. **C)** Quantitative analysis of changes in UCHL1 and UCHL3 levels by Western blotting. Relative protein expression (optical density) of the bands in panel **B**, normalized to α-tubulin. Each data point represents the mean ± SD (n = 4; * $P < 0.05$).

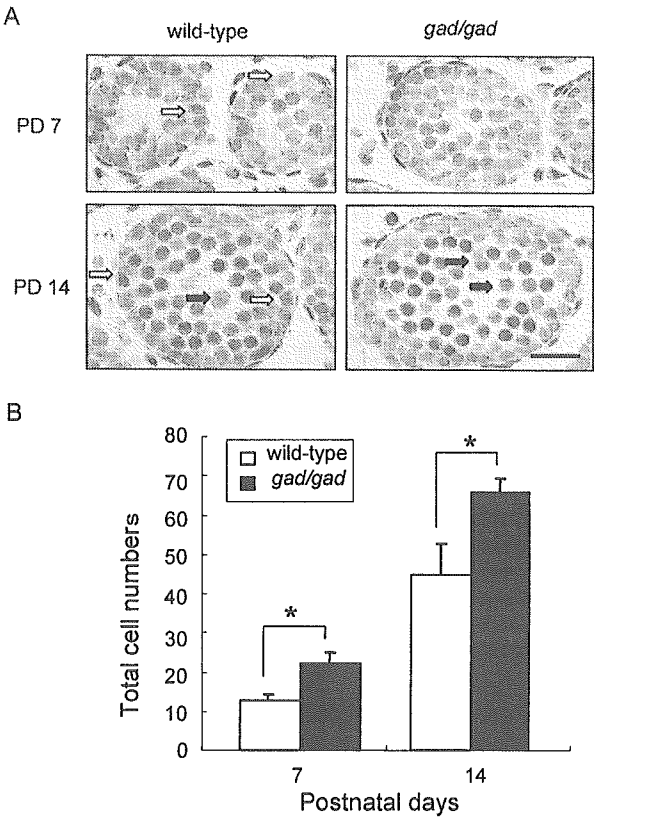

FIG. 2. **A)** Immunohistochemistry of UCHL1 and testicular morphology during the first round of spermatogenesis. UCHL1-positive germ cells in wild-type mice are indicated by open arrows. Spermatogonia and preleptotene spermatocytes (closed arrows) were more abundant and found further from the basement membrane in Postnatal Day (PD) 7 and 14 *gad* mice. Magnification ×200. Bar = 20 μm. **B)** The total number of germ cells in seminiferous tubules was significantly increased in and 7- and 14-day-old *gad* mice compared with wild-type mice (n = 4; * $P < 0.05$). Data represent mean ± SD.

based real-time quantitative RT-PCR (Fig. 1A). Despite the fact that the percentage of spermatogonia and Sertoli cells may be diluted by meiotic and postmeiotic germ cells after Day 14 [20], *Uchl1* expression was high in 14-day-old mice, in agreement with our previous findings.

Immunohistochemistry of UCHL1 and Quantitative Morphometric Assessment

Immunohistochemical analysis revealed UCHL1 expression in spermatogonia from wild-type mice but not *gad* mice (Fig. 2A). Preliminary examination of tubules from immature testes revealed an overproduction of germ cells in *gad* mice. At 7 and 14 days of age, the number of spermatogonia and preleptotene spermatocytes was significantly increased in *gad* mice compared with wild-type mice (Fig. 2A). The increase in the number of these cell types was further confirmed by quantitative analysis, which showed that the total number of testicular cells, including Sertoli cells, was significantly higher in 7- and 14-day-old *gad* mice (Fig. 2B).

TUNEL Staining of Apoptotic Germ Cells During the First Round of Spermatogenesis

To further investigate the mechanism underlying the observed differences in testicular cell numbers between wild-type and *gad* mice during the first round of spermatogenesis, we examined germ cell apoptosis in tissue sections from mice at 7, 14, 21, 28, and 35 days of age by TUNEL assay. During the first round of spermatogenesis, the total number of apoptotic cells in 20 circular seminiferous tubules decreased significantly (n = 4; $P < 0.05$) in gad mouse testes as compared with wild-type mice (Fig. 3A). Although germ cell apoptosis significantly increased at Day 14 in the testes of both wild-type and *gad* mice, *gad* mice had significantly fewer apoptotic germ cells (n = 4; $P < 0.05$) in seminiferous tubules (Fig. 3B).

Testicular Germ Cells of gad *Mice Are Resistant to Apoptosis-Inducing Conditions In Vitro*

Sertoli cells, which support germ cells, express UCHL1 [12]. To explore the viability of germ cells independently of the effect of Sertoli cells, testicular germ cells from 2-wk-old wild-type and *gad* mice were cultured in suspension for 5 days in the presence of 10% FBS. We then examined the resistance of these in vitro cell culture to apoptosis-inducing conditions. Although both wild-type and *gad* mouse cells were sensitive to apoptosis-inducing conditions, the *gad* mouse cells had comparatively greater viability (Fig. 4). Overall results clearly show that the absence of UCHL1 increase germ cell survival.

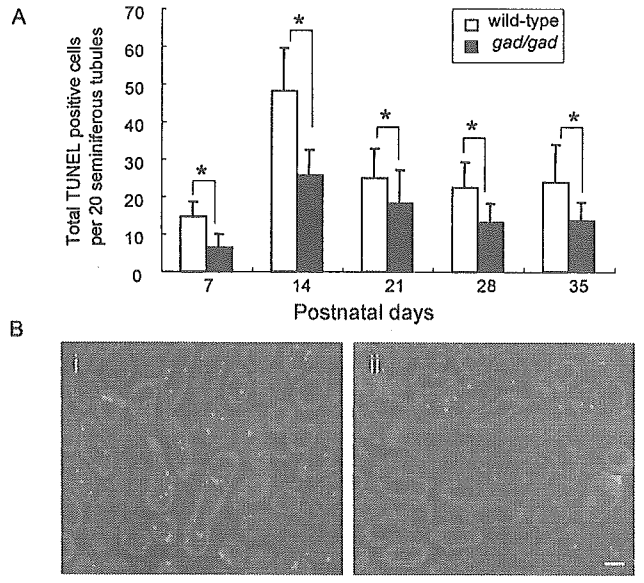

FIG. 3. A) The total TUNEL-positive germinal cells per 20 circular seminiferous tubules in wild-type and *gad* mice on various postnatal days. In each group, the data represent the mean ± SD (n = 4; * $P < 0.05$). B) The extent of apoptosis in 2-wk-old mice. i, wild-type mice; ii, *gad* mice. Green fluorescence, TUNEL-positive cells; red fluorescence, nuclei stained with propidium iodide. Magnification ×100. Bar = 30 μm.

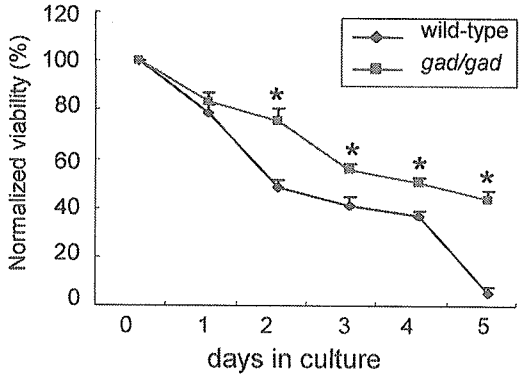

FIG. 4. In vitro survival of testicular germ cells. Testicular germ cells were isolated from wild-type and *gad* mice at 14 days of age. After culture, viability was determined using a Vi-Cell XR cell viability analyzer (Beckman Coulter). Viability at each time point was normalized to that at Day 0. Each data point represents the mean ± SD (n = 4; * $P < 0.05$).

Levels of Apoptotic Proteins During the First Round of Spermatogenesis

Germ cell apoptosis involves genes encoding various factors, such as *Trp53,* the *Bcl2* family, and *caspase,* which are targets for ubiquitination [29–31]. Our previous work demonstrated that the expression of antiapoptotic proteins (Bcl2 family and XIAP) is significantly elevated following cryptorchid stress in *gad* mice [22]. To explore whether the germ cell apoptotic wave is associated with changes in the levels of proteins known to be associated with cell death or survival, Western blot analysis was performed on testicular lysates obtained from 7-, 14-, 21-, 28-, and 35-day-old wild-type and *gad* mice (Fig. 5). Levels of TRP53 and Bax proteins were strikingly elevated in 7-day-old mice but barely detectable on Day 35. Caspase-3 was also strikingly elevated in 7-day-old mice. Since TRP53 modulates Bax expression [22, 32], the observed up-regulation of Bax is consistent with elevated TRP53 levels during the early apoptotic wave. Expression of the antiapoptotic protein Bcl-xL was weaker in immature compared with mature testes. Levels of TRP53, Bax, and caspase-3 proteins were significantly decreased in 7- and 14-day-old *gad* mice relative to the levels observed in wild-type testes (Fig. 5B). By contrast, the level of Bcl-xL protein appeared to be up-regulated earlier in *gad* mice (at 28 days) than in wild-type mice (at 35 days) (Fig. 5B).

Assessment of Cauda Epididymidis and Spermatozoa Morphology in gad *Mice*

The cauda epididymidis from wild-type and *gad* mice were weighed, and the sperm were collected and analyzed. The cauda epididymidis from *gad* mice weighed significantly less, likely resulting from the lower sperm concentration measured in *gad* mice (19.5×10^6/ml) compared with wild-type mice (23.6×10^6/ml) (Table 1). Furthermore, abnormal sperm morphology, including head and midpiece defects or a detached head, occurred significantly more often in *gad* mice (Table 1 and Fig. 6A). Immunocytochemical analysis showed that UCHL1 and ubiquitin were expressed in defective spermatozoa but not in normal spermatozoa (Fig. 6B). Ubiquitin, a marker for sperm abnormalities [33], was detected mainly in defective spermatozoa. However, despite a significantly elevated number of defective spermatozoa, ubiquitin expression in *gad* mouse spermatozoa was similar to that in wild-type mice (data not shown).

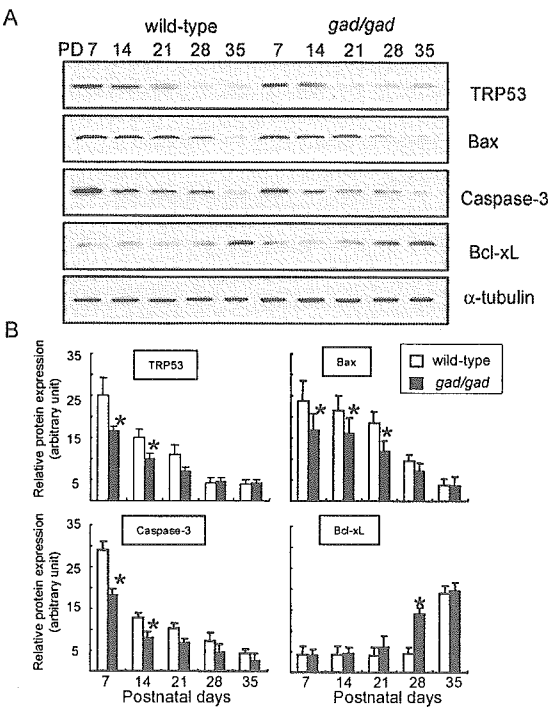

FIG. 5. A) Western blot analyses showing TRP53, Bax, caspase-3, and Bcl-xL levels in wild-type and *gad* mice during the first round of spermatogenesis. Protein (5 μg/lane) was prepared from whole testes at 7, 14, 21, 28, and 35 days of age. Blots were reprobed for α-tubulin to normalize for differences in the amount of protein loaded. Representative images of four independent experiments are shown. B) Quantitative Western blot analysis of changes in TRP53, Bax, caspase-3, and Bcl-xL levels. Relative protein expression (optical density) of the bands in panel A, normalized to α-tubulin. Each data point represents the mean ± SD (n = 4; * $P < 0.05$).

TABLE 1. Analysis of epididymal tail weight and sperm morphology (mean ± SD) in 10-week-old wild-type and *gad* mice.

	Tail weight (mg)	Sperm concentration (10^6/ml)	Defect (%)			
			Head	Midpiece	Principal piece	Detached head
wild-type	30.0 ± 0.8	23.6 ± 3.7	7.2 ± 1.5	2.4 ± 1.3	1.1 ± 0.2	2.0 ± 1.0
gad/gad	24.7 ± 1.1*	19.5 ± 3.3*	14.1 ± 2.8*	4.7 ± 1.5*	1.7 ± 0.6	3.7 ± 1.2*

* Significantly different from wild-type mice (n = 7; $P < 0.05$).

Spermatozoa Motility in gad *Mice*

We measured sperm motility parameters in wild-type and *gad* mice. Of the parameters assessed, MSP, PMP, VAP (μm/sec), VSL (μm/sec), and VCL (μm/sec) were significantly lower in *gad* mice. ALH (μm), linearity (%), and straightness (%) did not differ significantly between *gad* and wild-type mice (Fig. 7). Of the parameters we measured, the number of PMP differed most significantly between *gad* mice (24.4%) and wild-type mice (34.3%) (Fig. 7A).

DISCUSSION

Spermatogenesis is a highly complex process involving male germ cell proliferation and maturation from spermatogonia to spermatozoa [34]. Apoptosis is common during this process and is believed to play an important role in controlling germ cell numbers and eliminating defective germ cells that carry DNA mutations, thus ensuring the production of intact, functional spermatozoa [35–37]. Normally, germ cells are extremely sensitive to DNA damage, as such lesions are incompatible with the ultimate function of these cells [23, 24, 37]. The early apoptotic wave may result in early elimination of defective germ cells in which DNA alterations have occurred through chromosomal crossing over during the first meiotic division [23, 24, 37].

Several lines of evidence indicate that UCHL1 associates with monoubiquitin and that the monoubiquitin pool is reduced in *gad* mice relative to wild-type mice [18, 19, 22]. Furthermore, testes from UCHL1-deficient *gad* mice [22] and mice carrying the K48R mutation in ubiquitin [38] show resistance to cryptorchid-induced apoptosis, suggesting that ubiquitin is critical for modulating testicular germ cell death. Normally, damaged proteins are polyubiquitinated and degraded via the ubiquitin-proteasome system; however, if damaged proteins are not degraded as easily when monoubiquitin is either mutated or reduced [22, 38], then germinal cells may become resistant to programmed death. Our results with the *gad* mouse suggest that ubiquitin induction is important for regulating programmed germinal cell death that is normally observed during the first round of spermatogenesis. We have now shown that immature testes from *gad* mice are resistant to the massive wave of germinal cell apoptosis during the first round of spermatogenesis. The increased resistance of UCHL1-deficient germ cells to apoptosis-inducing conditions in vivo and in vitro suggests that UCHL1 is involved in spermatogenesis (Figs. 3 and 4). The activity of the ubiquitin-proteasome system may be required for specific transitions between multiple developmental cellular processes and sequential apoptosis during spermatogenesis [6, 7, 39]. In addition, the ubiquitin-proteasome system is required for the degradation or modification of numerous germ cell-specific proteins during different phases of spermatogenesis [39–41].

Early apoptosis in testicular germ cells is regulated by a complicated signal transduction pathway. The testes contain high levels of TRP53, Bcl2 family, and caspase-3 proteins, which are targets for ubiquitination [29–31, 42–45]. However, the involvement of the ubiquitin system in the regu-

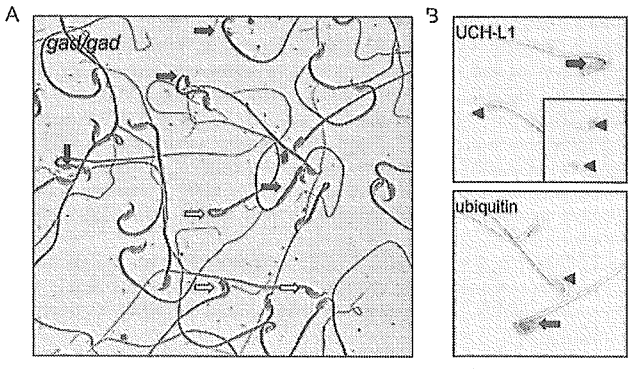

FIG. 6. A) Abnormal morphology of spermatozoa from *gad* mice. Spermatozoa were collected from the cauda epididymidis of 10-wk-old *gad* mice. Head defects (open arrows) and midpiece defects (closed arrows) are indicated. Magnification ×400. B) Immunocytochemistry of UCH-L1 and ubiquitin in wild-type and *gad* mice. UCHL1- and ubiquitin-positive spermatozoa (closed arrows) and normal spermatozoa (both negative, arrowheads) in wild-type mice are indicated. The inset shows an the image of spermatozoa from *gad* mice. Magnification ×1000.

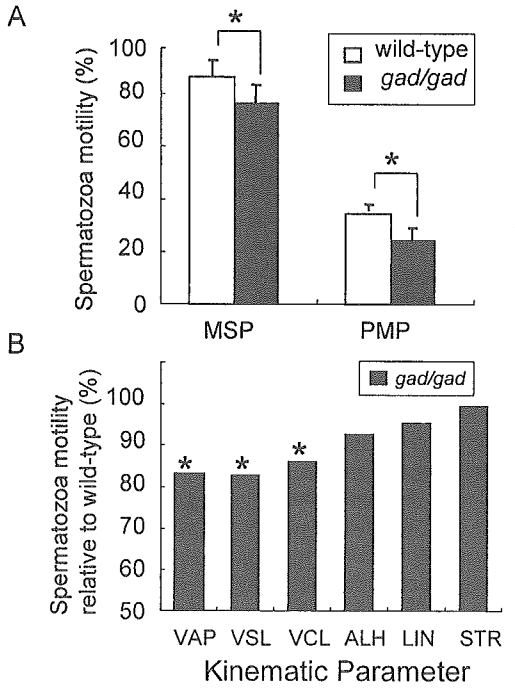

FIG. 7. Kinematic analysis of spermatozoa from the cauda epididymidis of 10-week-old wild-type and *gad* mice. A) Sperm motility. MSP, Percentage of motile sperm; PMP, Percentage of progressively motile sperm (n = 7; * $P < 0.05$). Data represent the mean ± SD. B) Movement characterization. VAP, Average path velocity (μm/sec); VSL, Straight-line velocity (μm/sec); VCL, Curvilinear velocity (μm/sec); ALH, Lateral head displacement (μm); LIN, Linearity (VSL/VCL × 100); STR, Straightness (VSL/VAP × 100). Data are expressed as a percentage of the values obtained for each parameter in wild-type mice (n = 7; * $P < 0.05$).

latory mechanisms of germ cell apoptosis has not been identified. A previous study showed that UCHL1-deficient *gad* mice express high levels of antiapoptotic proteins (Bcl2 family and XIAP) in the testis following cryptorchid-induced stress [22]. Alterations in the carefully maintained balance between the expression of apoptosis-inducing and apoptosis-protecting proteins may constitute one mechanism underlying the suppression of germ cell apoptosis observed in *gad* mice [46]. The decreased levels of TRP53, Bax, and caspase-3 observed in *gad* mice in this study are consistent with the suppression of germ cell apoptosis. In addition, the expression of the antiapoptotic protein Bcl-xL increased earlier in *gad* mice compared with wild-type mice. Therefore, the control of the apoptotic wave probably depends on variations in the balance between Bax and Bcl-xL [23, 47]. Analysis of the first round of spermatogenesis over time demonstrated a striking and massive wave of apoptotic germinal cells in 14-day-old mice (Fig. 3). High levels of UCHL1 protein were also observed at this age (Fig. 1) [20]. This early apoptotic wave was suppressed in the testes of *gad* mice, which had an abundance of germ cells compared with wild-type mice (Fig. 2). Moreover, the suppression of germ cell death is consistent with our previous report on cryptorchid stress injury in *gad* mice [22]. The testes of *gad* mice showed a phenotype similar to that of *Bax*-deficient mice or those overexpressing *Bcl2* or *Bcl-xL* [23, 25, 26]. Also, the testes of *Trp53*$^{-/-}$ mice exhibited a similar phenotype involving decreased germ cell apoptosis and an increased number of germ cells [48].

In the present study, we also characterized spermatozoa in *gad* mice with regard to the following reproductive endpoints: 1) the weight of reproductive organs, 2) the concentration of sperm cells, and 3) the motility and morphology of spermatozoa collected from the cauda epididymidis. The weight of cauda epididymidis from *gad* mice was significantly lower compared with that from wild-type mice. The concentration of sperm cells was also significantly lower, and most motility parameters of spermatozoa collected from the cauda epididymidis were affected in *gad* mice (Fig. 7). The significant decline in progressive forward motility, VAP, VSL, and VCL indicates that UCHL1 deficiency affects not only the ability of spermatozoa to move in the forward direction but also their vigor. In addition, the percentage of morphologically abnormal spermatozoa was significantly higher in *gad* mice (Table 1 and Fig. 6A).

Sperm production in the testis is a regulated balance between germ cell division and germ cell loss [26, 49], and there is emerging evidence that the ubiquitin-proteasome system may be central to the coordination of this process. For example, during spermatogenesis, the general activity of the ubiquitin-proteasome system is high, probably reflecting the requirement for massive degradation of cytoplasmic and nuclear proteins [6, 7, 50, 51]. Additionally, mutation of the ubiquitin-conjugating enzyme HR6B results in impaired spermatogenesis during nuclear condensation in spermatids [39, 41]. We found the fact that UCH-L1 associates with monoubiquitin in several lines of *gad* mice [18, 19, 22]. Furthermore, both proteins are expressed abundantly and at comparable levels in testis and the epididymis [11, 13, 14], suggesting that the functions of two proteins are important during spermatogenesis. Ubiquitin is present in defective spermatozoa, and proteins in these cells become ubiquitinated during epididymal passage (Fig. 6B) [11, 14, 33, 52, 53]. Furthermore, ubiquitination in the epididymis may trigger apoptotic mechanisms that recognize and eliminate abnormal spermatozoa [49, 54, 55].

Further study is required to elucidate the functional significance of the association between UCHL1 and ubiquitin during spermatozoa maturation in the epididymis. However, our observations suggest that UCHL1 may function to regulate sperm production and to ubiquitinate proteins in defective spermatozoa. Our present study demonstrates that UCHL1-deficient *gad* mice are resistant to the wave of germinal cell apoptosis that occurs during the first round of spermatogenesis and that these mice have defects in sperm production, motility, and morphology. These results suggest that UCHL1 functions in the early apoptotic wave during the first round of spermatogenesis and in the control of sperm quality during sperm maturation.

ACKNOWLEDGMENTS

We thank H. Kikuchi for technical assistance with tissue sections and M. Shikama for the care and breeding of animals.

REFERENCES

1. Ciechanover A, Finley D, Varshavsky A. Ubiquitin dependence of selective protein degradation demonstrated in the mammalian cell cycle mutant ts85. Cell 1984; 37:57–66.
2. Glotzer M, Murray AW, Kirschner MW. Cyclin is degraded by the ubiquitin pathway. Nature 1991; 349:132–138.
3. Strous GJ, Govers R. The ubiquitin-proteasome system and endocytosis. J Cell Sci 1999; 112(pt 10):1417–1423.
4. Wilkinson KD. Regulation of ubiquitin-dependent processes by deubiquitinating enzymes. FASEB J 1997; 11:1245–1256.
5. Hershko A, Ciechanover A. The ubiquitin system. Annu Rev Biochem 1998; 67:425–479.
6. Baarends WM, Roest HP, Grootegoed JA. The ubiquitin system in gametogenesis. Mol Cell Endocrinol 1999; 151:5–16.
7. Baarends WM, van der Laan R, Grootegoed JA. Specific aspects of the ubiquitin system in spermatogenesis. J Endocrinol Invest 2000; 23:597–604.
8. Ciechanover A. The ubiquitin-proteasome pathway: on protein death and cell life. EMBO J 1998; 17:7151–7160.
9. Weissman AM. Themes and variations on ubiquitylation. Nat Rev Mol Cell Biol 2001; 2:169–178.
10. Wing SS. Deubiquitinating enzymes—the importance of driving in reverse along the ubiquitin-proteasome pathway. Int J Biochem Cell Biol 2003; 35:590–605.
11. Fraile B, Martin R, De Miguel MP, Arenas MI, Bethencourt FR, Peinado F, Paniagua R, Santamaria L. Light and electron microscopic immunohistochemical localization of protein gene product 9.5 and ubiquitin immunoreactivities in the human epididymis and vas deferens. Biol Reprod 1996; 55:291–297.
12. Kon Y, Endoh D, Iwanaga T. Expression of protein gene product 9.5, a neuronal ubiquitin C-terminal hydrolase, and its developing change in sertoli cells of mouse testis. Mol Reprod Dev 1999; 54:333–341.
13. Kwon J, Kikuchi T, Setsuie R, Ishii Y, Kyuwa S, Yoshikawa Y. Characterization of the testis in congenitally ubiquitin carboxy-terminal hydrolase-1 (Uch-L1) defective (gad) mice. Exp Anim 2003; 52:1–9.
14. Martin R, Santamaria L, Fraile B, Paniagua R, Polak JM. Ultrastructural localization of PGP 9.5 and ubiquitin immunoreactivities in rat ductus epididymidis epithelium. Histochem J 1995; 27:431–439.
15. Pickart CM, Rose IA. Ubiquitin carboxyl-terminal hydrolase acts on ubiquitin carboxyl-terminal amides. J Biol Chem 1985; 260:7903–7910.
16. Liu Y, Fallon L, Lashuel HA, Liu Z, Lansbury PT, Jr. The UCH-L1 gene encodes two opposing enzymatic activities that affect alpha-synuclein degradation and Parkinson's disease susceptibility. Cell 2002; 111:209–218.
17. Liu Y, Lashuel HA, Choi S, Xing X, Case A, Ni J, Yeh LA, Cuny GD, Stein RL, Lansbury PT, Jr. Discovery of inhibitors that elucidate the role of UCH-L1 activity in the H1299 lung cancer cell line. Chem Biol 2003; 10:837–846.
18. Osaka H, Wang YL, Takada K, Takizawa S, Setsuie R, Li H, Sato Y, Nishikawa K, Sun YJ, Sakurai M, Harada T, Hara Y, Kimura I, Chiba S, Namikawa K, Kiyama H, Noda M, Aoki S, Wada K. Ubiquitin carboxy-terminal hydrolase L1 binds to and stabilizes monoubiquitin in neuron. Hum Mol Genet 2003; 12:1945–1958.

19. Harada T, Harada C, Wang YL, Osaka H, Amanai K, Tanaka K, Takizawa S, Setsuie R, Sakurai M, Sato Y, Noda M, Wada K. Role of ubiquitin carboxy terminal hydrolase-L1 in neural cell apoptosis induced by ischemic retinal injury in vivo. Am J Pathol 2004; 164:59–64.
20. Kwon J, Wang YL, Setsuie R, Sekiguchi S, Sakurai M, Sato Y, Lee WW, Ishii Y, Kyuwa S, Noda M, Wada K, Yoshikawa Y. Developmental regulation of ubiquitin C-terminal hydrolase isozyme expression during spermatogenesis in mice. Biol Reprod 2004; 71:515–521.
21. Saigoh K, Wang YL, Suh JG, Yamanishi T, Sakai Y, Kiyosawa H, Harada T, Ichihara N, Wakana S, Kikuchi T, Wada K. Intragenic deletion in the gene encoding ubiquitin carboxy-terminal hydrolase in gad mice. Nat Genet 1999; 23:47–51.
22. Kwon J, Wang YL, Setsuie R, Sekiguchi S, Sato Y, Sakurai M, Noda M, Aoki S, Yoshikawa Y, Wada K. Two closely related ubiquitin C-terminal hydrolase isozymes function as reciprocal modulators of germ cell apoptosis in cryptorchid testis. Am J Pathol 2004; 165: 1367–1374.
23. Rodriguez I, Ody C, Araki K, Garcia I, Vassalli P. An early and massive wave of germinal cell apoptosis is required for the development of functional spermatogenesis. EMBO J 1997; 16:2262–2270.
24. Jahnukainen K, Chrysis D, Hou M, Parvinen M, Eksborg S, Soder O. Increased apoptosis occurring during the first wave of spermatogenesis is stage-specific and primarily affects midpachytene spermatocytes in the rat testis. Biol Reprod 2004; 70:290–296.
25. Furuchi T, Masuko K, Nishimune Y, Obinata M, Matsui Y. Inhibition of testicular germ cell apoptosis and differentiation in mice misexpressing Bcl-2 in spermatogonia. Development 1996; 122:1703–1709.
26. Russell LD, Chiarini-Garcia H, Korsmeyer SJ, Knudson CM. Bax-dependent spermatogonia apoptosis is required for testicular development and spermatogenesis. Biol Reprod 2002; 66:950–958.
27. Slott VL, Suarez JD, Perreault SD. Rat sperm motility analysis: methodologic considerations. Reprod Toxicol 1991; 5:449–458.
28. Goyal HO, Braden TD, Mansour M, Williams CS, Kamaleldin A, Srivastava KK. Diethylstilbestrol-treated adult rats with altered epididymal sperm numbers and sperm motility parameters, but without alterations in sperm production and sperm morphology. Biol Reprod 2001; 64:927–934.
29. Chipuk JE, Green DR. Cytoplasmic p53: Bax and forward. Cell Cycle 2004; 3:429–431.
30. Dimmeler S, Breitschopf K, Haendeler J, Zeiher AM. Dephosphorylation targets Bcl-2 for ubiquitin-dependent degradation: a link between the apoptosome and the proteasome pathway. J Exp Med 1999; 189:1815–1822.
31. Suzuki Y, Nakabayashi Y, Takahashi R. Ubiquitin-protein ligase activity of X-linked inhibitor of apoptosis protein promotes proteasomal degradation of caspase-3 and enhances its anti-apoptotic effect in Fas-induced cell death. Proc Natl Acad Sci U S A 2001; 98:8662–8667.
32. Selvakumaran M, Lin HK, Miyashita T, Wang HG, Krajewski S, Reed JC, Hoffman B, Liebermann D. Immediate early upregulation of bax expression by p53 but not TGF beta 1: a paradigm for distinct apoptotic pathways. Oncogene 1994; 9:1791–1798.
33. Sutovsky P, Moreno R, Ramalho-Santos J, Dominko T, Thompson WE, Schatten G. A putative, ubiquitin-dependent mechanism for the recognition and elimination of defective spermatozoa in the mammalian epididymis. J Cell Sci 2001; 114:1665–1675.
34. de Kretser DM, Loveland KL, Meinhardt A, Simorangkir D, Wreford N. Spermatogenesis. Hum Reprod 1998; 13(suppl 1):1–8.
35. Gosden R, Spears N. Programmed cell death in the reproductive system. Br Med Bull 1997; 53:644–661.
36. Matsui Y. Regulation of germ cell death in mammalian gonads. APMIS 1998; 106:142–147Ascussion 147–148.
37. Print CG, Loveland KL. Germ cell suicide: new insights into apoptosis during spermatogenesis. Bioessays 2000; 22:423–430.
38. Rasoulpour RJ, Schoenfeld HA, Gray DA, Boekelheide K. Expression of a K48R mutant ubiquitin protects mouse testis from cryptorchid injury and aging. Am J Pathol 2003; 163:2595–2603.
39. Baarends WM, Wassenaar E, Hoogerbrugge JW, van Cappellen G, Roest HP, Vreeburg J, Ooms M, Hoeijmakers JH, Grootegoed JA. Loss of HR6B ubiquitin-conjugating activity results in damaged synaptonemal complex structure and increased crossing-over frequency during the male meiotic prophase. Mol Cell Biol 2003; 23:1151–1162.
40. Baarends WM, Hoogerbrugge JW, Roest HP, Ooms M, Vreeburg J, Hoeijmakers JH, Grootegoed JA. Histone ubiquitination and chromatin remodeling in mouse spermatogenesis. Dev Biol 1999; 207: 322–333.
41. Roest HP, van Klaveren J, de Wit J, van Gurp CG, Koken MH, Vermey M, van Roijen JH, Hoogerbrugge JW, Vreeburg JT, Baarends WM, Bootsma D, Grootegoed JA, Hoeijmakers JH. Inactivation of the HR6B ubiquitin-conjugating DNA repair enzyme in mice causes male sterility associated with chromatin modification. Cell 1996; 86: 799–810.
42. Marshansky V, Wang X, Bertrand R, Luo H, Duguid W, Chinnadurai G, Kanaan N, Vu MD, Wu J. Proteasomes modulate balance among proapoptotic and antiapoptotic Bcl-2 family members and compromise functioning of the electron transport chain in leukemic cells. J Immunol 2001; 166:3130–3142.
43. Oren M. Regulation of the p53 tumor suppressor protein. J Biol Chem 1999; 274:36031–36034.
44. Orlowski RZ. The role of the ubiquitin-proteasome pathway in apoptosis. Cell Death Differ 1999; 6:303–313.
45. Yang Y, Yu X. Regulation of apoptosis: the ubiquitous way. FASEB J 2003; 17:790–799.
46. Beumer TL, Roepers-Gajadien HL, Gademan IS, Lock TM, Kal HB, De Rooij DG. Apoptosis regulation in the testis: involvement of Bcl-2 family members. Mol Reprod Dev 2000; 56:353–359.
47. Borner C. The Bcl-2 protein family: sensors and checkpoints for life-or-death decisions. Mol Immunol 2003; 39:615–647.
48. Yin Y, Stahl BC, DeWolf WC. Morgentaler A. p53-mediated germ cell quality control in spermatogenesis. Dev Biol 1998; 204:165–171.
49. Sutovsky P. Ubiquitin-dependent proteolysis in mammalian spermatogenesis, fertilization, and sperm quality control: killing three birds with one stone. Microsc Res Tech 2003; 61:88–102.
50. Rajapurohitam V, Bedard N, Wing SS. Control of ubiquitination of proteins in rat tissues by ubiquitin conjugating enzymes and isopeptidases. Am J Physiol Endocrinol Metab 2002; 282:E739–E745.
51. Rajapurohitam V, Morales CR, El-Alfy M, Lefrancois S, Bedard N, Wing SS. Activation of a UBC4-dependent pathway of ubiquitin conjugation during postnatal development of the rat testis. Dev Biol 1999; 212:217–228.
52. Lippert TH, Seeger H, Schieferstein G, Voelter W. Immunoreactive ubiquitin in human seminal plasma. J Androl 1993; 14:130–131.
53. Sutovsky P, Terada Y, Schatten G. Ubiquitin-based sperm assay for the diagnosis of male factor infertility. Hum Reprod 2001; 16:250–258.
54. Sinha Hikim AP, Swerdloff RS. Hormonal and genetic control of germ cell apoptosis in the testis. Rev Reprod 1999; 4:38–47.
55. Sutovsky P, Hauser R, Sutovsky M. Increased levels of sperm ubiquitin correlate with semen quality in men from an andrology laboratory clinic population. Hum Reprod 2004; 19:628–638.